PHYSICAL REVIEW D VOLUME 35, NUMBER 11 1 JUNE 1987

Superheavy-quarkonium production and decays: A new Higgs-boson signal

V. Barger
Physics Department, University of Wisconsin, Madison, Wisconsin 53706

E. W. N. Glover
Physics Department, University of Wisconsin, Madison, Wisconsin 53706
and Cavendish Laboratory, University of Cambridge, Cambridge CB3 0HE, England

K. Hikasa
Physics Department, University of Wisconsin, Madison, Wisconsin 53706
and National Laboratory for High Energy Physics (KEK), Tsukuba, Ibaraki 305, Japan

W.-Y. Keung
Physics Department, University of Illinois, Chicago, Illinois 60680

M. G. Olsson, C. J. Suchyta III, and X. R. Tata
Physics Department, University of Wisconsin, Madison, Wisconsin 53706
(Received 27 January 1987)

We study the production and subsequent decays of the S- and P-wave quarkonium states of a heavy quark that may be produced at a multi-TeV hadron collider. Our considerations are focused on the lighter member of a fourth-generation doublet, for which the weak decays of the quark are expected to be suppressed by mixing angles. For quarkonium masses $\lesssim 1$ TeV, the dominant production is via gluon fusion. In addition to the decay channels that are present in the charm and bottom systems, heavy quarkonia can decay into W^+W^-, Z^0Z^0, and $Z^0\gamma$ pairs. Furthermore, the latter decay rates may be enhanced due to couplings of the heavy quarks to the longitudinal components of the gauge bosons. We assess the prospects for discovery of a new heavy quark via its bound-state decays. Quarks with masses up to ≈ 100 GeV can be found from the decay of the 1^{--} state (ψ) into lepton pairs. If the decay of the pseudoscalar quarkonium state into a Z boson and a Higgs boson is kinematically allowed, there is a rather clean signal for the Higgs boson, even for the intermediate-mass Higgs boson with $2m_t < m_H < 2M_W$. Furthermore, $H\gamma$ and HH pairs would also be present at fairly large rates.

I. INTRODUCTION

The first signals in hadronic collisions for charm and bottom quarks were the leptonic decays of the J/ψ and Υ bound states. Hence it is of particular interest to examine the possibilities for discovery of new heavy-quark flavors at hadronic colliders through the decays of their quarkonium bound states. The $t\bar{t}$ quarkonium signals were examined previously[1] and found to be rather elusive. However, in a recent Letter[2] we showed that the prospects for simultaneously identifying a fourth-generation quarkonium state and the Higgs boson at supercollider energies were very promising, due to the possible dominance of the distinctive decay mode $\eta(Q\bar{Q})\to ZH$ of the pseudoscalar bound state η into a Z boson and a Higgs boson. In this paper we make a thorough study of production and decays of $\eta(0^{-+})$, $\psi(1^{--})$, $\chi(0^{++},1^{++},2^{++})$, and $h(1^{+-})$ superheavy quarkonium states.

Quarkonium states with masses $M_{Q\bar{Q}} \lesssim 1$ TeV would be produced with substantial cross sections at hadron supercolliders with a center-of-mass energy of 10—40 TeV. For these energies, the gg luminosity exceeds the $q\bar{q}$ luminosity by a factor $\gtrsim 50$, and gluon fusion is the dominant source of quarkonium production. The pseudoscalar state $\eta(Q\bar{Q})$ and the scalar and tensor P-wave states $\chi_0(Q\bar{Q})$ and $\chi_2(Q\bar{Q})$ couple directly to two gluons and are directly produced via the gluon-fusion mechanism. The vector state $\psi(Q\bar{Q})$ and the spin-1 P-wave states $\chi_1(Q\bar{Q})$ and $h(Q\bar{Q})$ couple only to the three-gluon or $q\bar{q}g$ system. Here the dominant production mechanism is the process[3] $gg\to\psi g$. This is so even though the decay width for $\psi\to q\bar{q}$ exceeds that for $\psi\to ggg$ because the gluon lumi-

nosity is far greater than the quark luminosity for quarkonium masses $M_{Q\bar{Q}} \lesssim 1$ TeV. We ignore the possibility $M_\psi \simeq M_Z$, which has been considered elsewhere.[4] The quarkonium production cross sections are proportional to the quarkonium decay width into gluons, which can be estimated within the framework of nonrelativistic potential models.

Heavy-quarkonium decays lead to a variety of interesting final-state topologies. In addition to conventional signals from $\eta, \chi_0, \chi_2 \to \gamma\gamma$ and $\psi \to l^+ l^-$ decays, potentially interesting new signals for heavy quarkonium are the decays into gauge-boson pairs W^+W^-, Z^0Z^0, and $Z^0\gamma$ and also into Z^0+Higgs boson. The latter decay mode may make it possible to search for the intermediate-mass Higgs boson. The proposed U.S. Superconducting Super Collider (SSC) is particularly well suited for searching for the $\eta \to ZH$ signal for two reasons: (i) It would be a high-luminosity machine, making searches for relatively rare but distinctive signatures possible, (ii) the cross section for pseudoscalar-quarkonium production is large because of the high gluon luminosity at very high energy. Quarkonium decays may also be a source of sequential-heavy-lepton pairs.

Central to our considerations is the assumption that the spectator decay of the heavy-quark constituents in the quarkonium are suppressed. We argue that this is likely to be the case for the lighter member of a fourth-generation doublet, if the intergeneration mixing is small.

Our analysis naturally divides into several parts: (i) potential-model wave functions (Sec. II); (ii) calculation of quarkonium production cross sections (Sec. III); (iii) partial widths and branching fractions for the various quarkonium decay modes (Sec. IV); (iv) physics signatures and backgrounds (Sec. V).

A discussion of the calculational methods used in evaluating bound-state decay rates is given in Appendix A. Appendix B contains an explicit illustration of the computation for cases $\mathcal{O} \to ZZ$.

The considerations of this paper can also be applied to quarkonia formed from isosinglet heavy quarks that occur in the 27-dimensional representation of E_6, with some modifications in the decay calculations. We should also mention that although we confine our analysis to heavy-quarkonium signatures at the SSC, the novel decay modes discussed in Sec. IV may also be relevant to heavy-quarkonium production at a very-high-energy electron-positron collider.

II. POTENTIAL MODELS

The decay widths and production cross sections of quarkonium states depend crucially on the quarkonium wave function. Although the quark-antiquark potential, from which the wave functions can be derived, is given by one-gluon exchange at short distances and is calculable, the intermediate distance part of the potential must be inferred from the existing charmonium and b-quarkonium data. The calculation of the wave functions of superheavy quarkonium require an extrapolation far from the presently observable regime, so the results could be sensitive to the choice of interquark potential model. Integrating the nonrelativistic Schrödinger equation by parts[5] and applying the usual boundary conditions at $r=0$ and ∞, we can relate the quarkonium wave functions squared at the origin to the derivative of the potential by

$$|R_S(0)|^2 = m_Q \left\langle \frac{dV}{dr} \right\rangle , \tag{2.1}$$

$$|R'_P(0)|^2 = \frac{m_Q}{9} \left\langle \frac{1}{r^2}\frac{dV}{dr} + 4(E-V)\frac{}{r^3} \right\rangle . \tag{2.2}$$

Here $\langle\ \rangle$ denotes an expectation value, $E = M_{Q\bar{Q}} - 2m_Q$, and $R_S(0)$ and $R'_P(0)$ are, respectively, the radial wave function of the S state and the derivative of the radial wave function for the P state evaluated at $r=0$. Because of the monotonicity of the potential, the quarkonium wave functions at the origin are determined mainly by the size of the quarkonium which is roughly the size of the Bohr radius $(\alpha_s m_Q)^{-1} \sim 10/m_Q$.

We have considered the following potential-model choices.

(1) Coulomb potential. In this case the short-distance part of the potential

$$V(r) = -\frac{4}{3}\frac{\alpha_s(m_Q{}^2)}{r} \tag{2.3}$$

is assumed to dominate, with a running strong coupling α_s given by Eq. (2.11) below, evaluated at a scale m_Q. The wave functions can be exactly calculated. For the lowest S and P states, we have $|R_S(0)|^2 = 4(\frac{2}{3}\alpha_s m_Q)^3$ and $|R'_P(0)|^2 = \frac{1}{24}(\frac{2}{3}\alpha_s m_Q)^5$. This approximation slightly underestimates $|R_S(0)|^2$ but more seriously underestimates $|R'_P(0)|^2$ compared to more realistic potentials which include the long-range part. This is because the confinement force pushes in the wave functions relative to the case of the Coulomb potential; see Eqs. (2.1) and (2.2).

(2) Cornell potential.[6] This potential is parametrized by

$$V(r) = -k/r + ar \tag{2.4}$$

with the constants k and a fixed by $c\bar{c}$ and $b\bar{b}$ quarkonium data. The empirical coefficient of the short-distance part, $k \sim 0.5$, is much larger than the perturbative QCD expectation, $\frac{4}{3}\alpha_s \sim 0.1$–$0.2$, so the wave functions at the origin for superheavy quarkonia are considerably overestimated.

(3) Richardson potential.[7] This model incorporates the asymptotically free short-distance behavior and a linear confinement potential at large distances with an economical choice of parametrization in momentum space:

$$V(Q) = -\frac{4}{3}\frac{12\pi}{33-2N_f}\frac{1}{Q^2}\frac{1}{\ln(1+Q^2/\Lambda^2)} . \tag{2.5}$$

However, a value of $\Lambda \simeq 400$ MeV is necessary to reproduce the large-distance string tension; hence the superheavy-quarkonia decay widths may be somewhat overestimated.

(4) Wisconsin potential.[8] This model bridges the perturbative QCD behavior at short distance and linear confinement at large distance with a flexible parametrization for the intermediate region so that the short- and long-

distance parameters are not closely correlated. The potential is

$$V(r)=V_S(r)+V_I(r)+ar\ , \tag{2.6}$$

where $V_S(r)=-4\alpha_s(r)/3r$ with $\alpha_s(r)$ a regularized version of the two-loop perturbative coupling constant in which the Landau zero is pushed off to infinity. The intermediate potential $V_I(r)=r(c_1+c_2r)e^{-r/r_0}$ is a rather arbitrarily chosen form subject to the requirements that it vanish at small and large radii. In a fit to the $c\bar{c}$ and $b\bar{b}$ data the value $\Lambda_{\overline{\rm MS}}\sim 250$ MeV is preferred ($\overline{\rm MS}$ denotes the modified minimal-subtraction scheme). This potential is presumably the most realistic and hopefully it yields a reliable estimate of the wave function of superheavy quarkonium at the origin. The short-distance behavior of both the Wisconsin and Richardson potentials is $(r\ln ar)^{-1}$ with the main difference being how they match onto the confining region.

The four potentials are shown for the sake of comparison in Fig. 1. Although the potentials look similar in the ψ and Υ regions, they differ markedly for large values of m_Q and so can yield quite different results in calculations involving heavy quarkonia.

Figure 2(a) shows the square of the radial wave function at the origin in units of $m_Q{}^2$ of the lowest S state. The square of the derivative of the wave function for the lowest P state is shown in Fig. 2(b). At large m_Q $|R_S(0)|^2$ and $|R_P'(0)|^2$ scale as $m_Q{}^3$ and $m_Q{}^5$ for the Cornell potential, similar to the Coulomb potential, whereas they grow much more slowly for the Richardson and Wisconsin potentials.

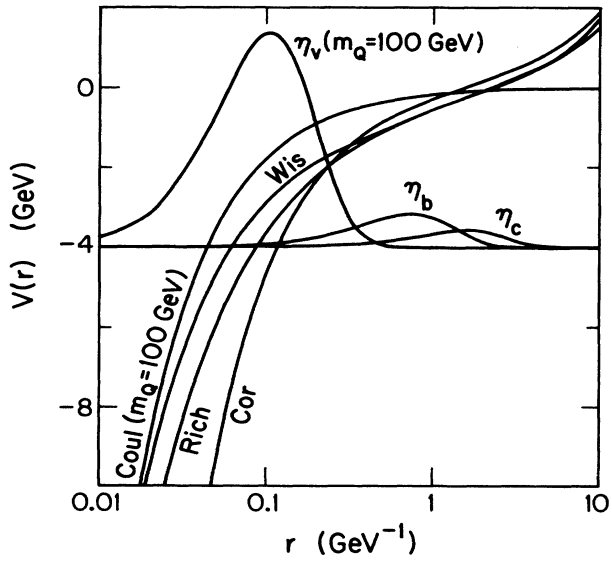

FIG. 1. Comparison of four QCD-motivated quarkonium potentials. The Coulomb, Cornell, Richardson, and Wisconsin potentials are labeled Coul, Cor, Rich, and Wis, respectively. Also shown is the S-wave function for the charm quark, bottom quark, and a new heavy quark with $m_Q=100$ GeV. In the curve marked Coul, α_s is evaluated at scale $m_Q{}^2$. Notice that the b-quarkonium and charmonium wave functions do not probe the short-range part of the potential.

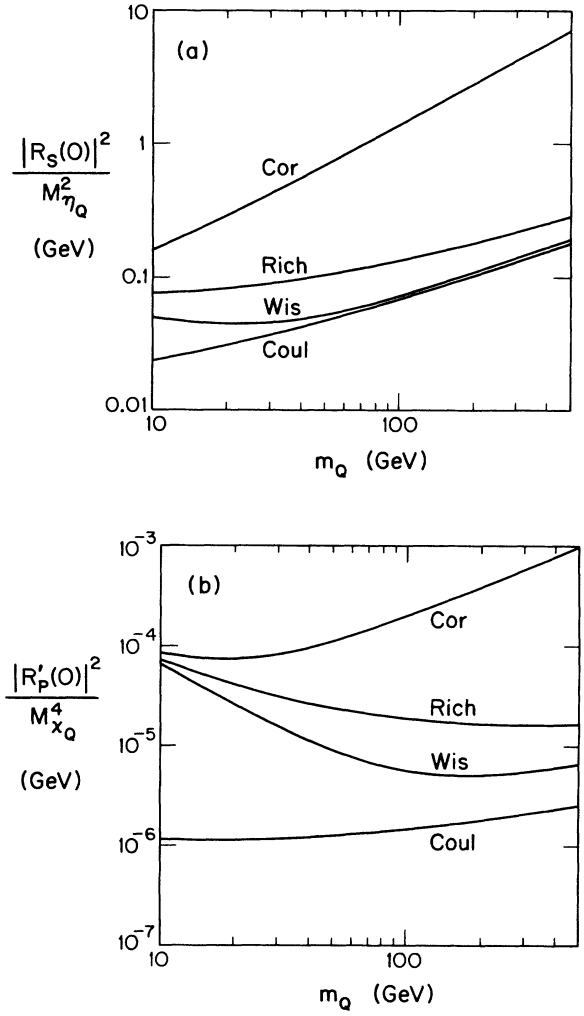

FIG. 2. (a) The S-wave radial wave function squared divided by $M_{\eta_Q}{}^2$ and (b) the derivative of P-wave function squared divided by $M_{\chi_Q}{}^4$ as a function of the mass of the heavy quark, m_Q. Notice that for large quark masses, the Coulomb wave functions are similar to those of the Wisconsin potential for S waves though the difference is quite large for P waves.

The partial widths into gluons of the various quarkonium states can be readily calculated and are given by[9]

$$\Gamma(\eta\to gg)=\frac{8\alpha_s{}^2}{3M_\eta{}^2}|R_S(0)|^2\ , \tag{2.7}$$

$$\Gamma(\psi\to 3g)=\frac{40(\pi^2-9)\alpha_s{}^3}{81\pi M_\psi{}^2}|R_S(0)|^2\ , \tag{2.8}$$

$$\Gamma(\chi_0\to gg)=\frac{96\alpha_s{}^2}{M_\chi{}^4}|R_P'(0)|^2\ , \tag{2.9}$$

$$\Gamma(\chi_2\to gg)=\tfrac{4}{15}\Gamma(\chi_0\to gg)\ . \tag{2.10}$$

For the strong coupling α_s, we take

$$\alpha_s = \frac{12\pi}{(33-2N_f)\ln(m_Q^2/\Lambda^2)} \tag{2.11}$$

with $N_f=6$ and $\Lambda=0.12$ GeV; this corresponds to $\Lambda(N_f=4)\sim 0.3$ GeV. The gluonic widths of Eqs. (2.7) and (2.9) are shown in Figs. 3(a) and 3(b) as a function of the mass of the quarkonium. The Cornell potential gives much larger values than the more realistic Richardson and Wisconsin potentials for large quark masses. It is instructive to note that for the latter potentials, the gluonic width is almost constant for χ_0 and increases rather slowly with m_Q for η. These widths will be used in Sec. III to estimate quarkonium production.

There are two potential model effects which will further increase the signals from the decay of quarkonia at the SSC.

(i) Because the relativistic kinetic energy is smaller[8] than its nonrelativistic counterpart, the relativistic potential energy must increase to keep the energy of the state fixed at a given level. The classical turning point moves inward, resulting in a larger wave function at the origin. The effect of this *kinetic-energy correction* is $\sim 10\%$ which may be as expected since $\alpha_s \sim 0.1$. More importantly, relativistic spin splitting results in larger wave functions at the origin for the lower-lying members of an orbital angular momentum multiplet; the lower state's wave function is compressed since the effective potential is more attractive. Wave-function enhancement factors due to this correction are in the range 20—50%, the bulk of which is due to relativistic spin effects.

(ii) For a given quarkonium state, there are $N_s \simeq 2(m_Q/1.5\ \text{GeV})^{1/2}$ sharp radial excitations with the same quantum numbers that all lie within a few GeV of one another.[10] Since these can all be produced via gluon fusion, the resulting cross sections may be enhanced by a factor

$$\epsilon_{\mathcal{O}} = \sum_{n=1}^{N_s} \Gamma(\mathcal{O}_n \to \text{gluons})/\Gamma(\mathcal{O}_1 \to \text{gluons}) \ .$$

The value of $\epsilon_{\mathcal{O}}$ depends on the potential as shown in Fig. 4(a) for η_Q. For the Cornell and Coulomb potentials, $\epsilon_{\mathcal{O}} \simeq 1.2$ as can be calculated from the $1/n^3$ falloff of the radial wave functions squared and is larger for the Wisconsin or Richardson potentials. The corresponding results for P waves are shown in Fig. 4(b).

We should note, however, that one cannot scale the cross sections for any given final state by $\epsilon_{\mathcal{O}}$ since the radial excitations can also cascade down to lower states either radiatively or hadronically. Because the branching ratios into various final states for different quarkonia are quite different, it is not correct to simply scale the various cross sections by the factor $\epsilon_{\mathcal{O}}$. Rather, the figure is only indicative of the sort of enhancements that may occur due to radial excitations. On the other hand, if a single decay such as ZH is dominant the radial enhancement factor is significant.

To be conservative, we ignore both relativistic and radial enhancement factors in the remainder of this paper.

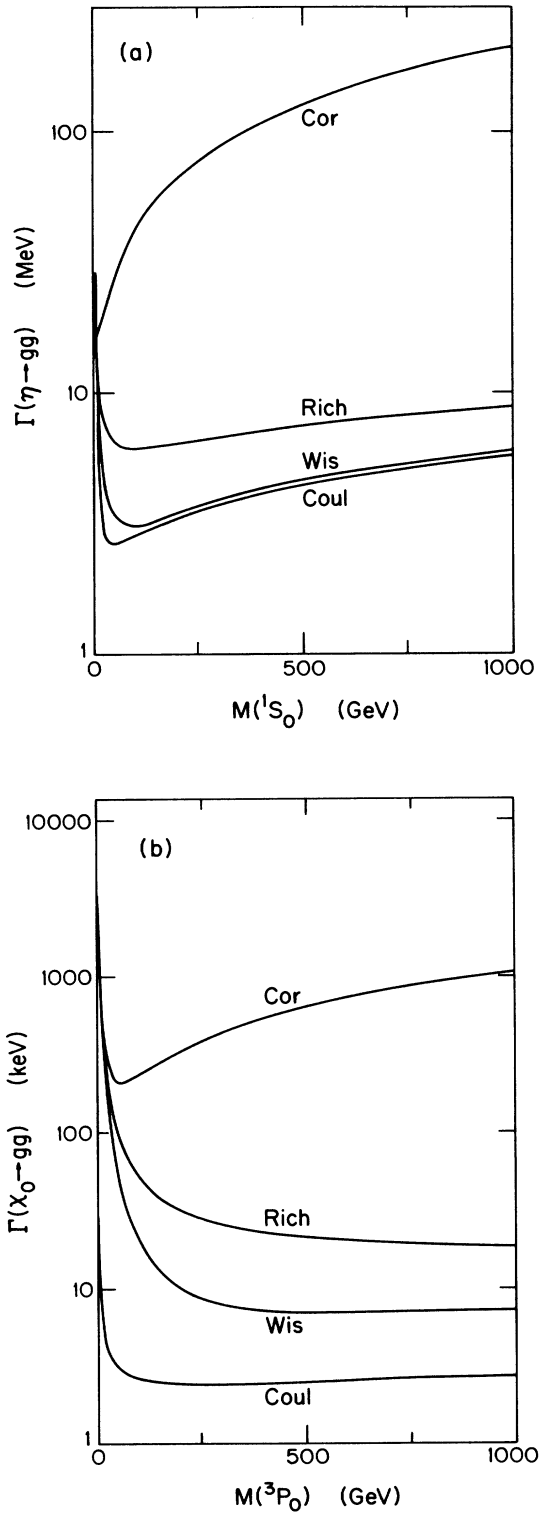

FIG. 3. The partial width (a) for $\eta_Q \to gg$ and (b) $\chi_{0Q} \to gg$ as a function of M_{η_Q}. The Cornell potential overestimates the width and hence the production of η_Q and $\chi_{0,2Q}$ in hadronic collisions. The width for $\chi_2 \to gg$ may be obtained by multiplying that in (b) by $\frac{4}{15}$.

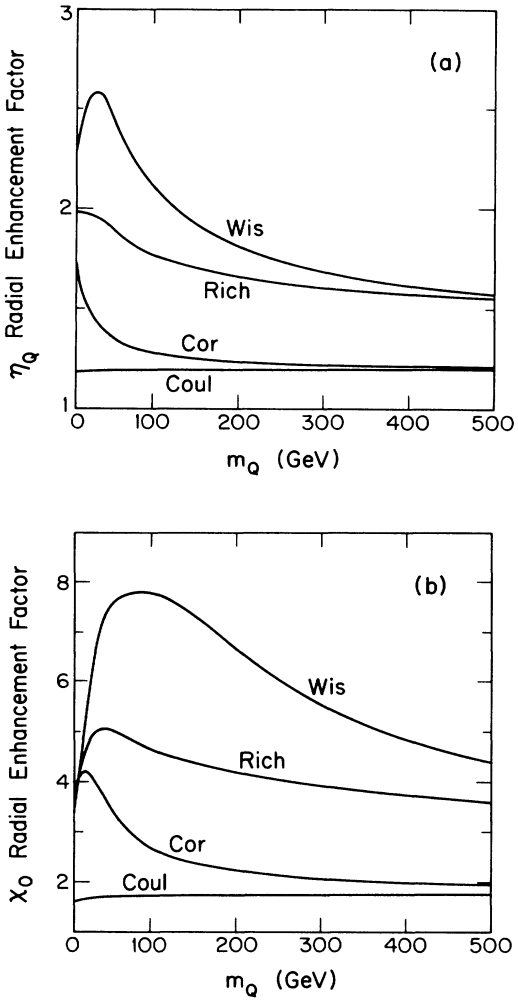

FIG. 4. The enhancement for (a) η_Q production and (b) χ_{0Q} production due to production of the radial excitations of the $^1S_0$ and $^3P_0$ states for the different potentials discussed in the text. Note that the Cornell and Coulomb potentials asymptotically approach the same value since they both have the same behavior for the short-range part of the potential.

III. PRODUCTION

Two alternative perturbative QCD approaches have been used in the past to calculate quarkonium production cross sections. One uses semilocal duality arguments to obtain the quarkonium cross section as a fraction of the heavy-quark pair-production cross section.[11,12] When the mass of the $Q\bar{Q}$ system is below the open flavor threshold $2M(Q\bar{q})$, the system is supposed to form a quarkonium. However, there is a large ambiguity in this procedure. First, the total quarkonium cross section is a small fraction of the $Q\bar{Q}$ cross section and is sensitive to the somewhat arbitrary choice of the light-quark mass. Second, duality arguments do not specify the relative abundance of the various quarkonium states.

The other method[13,14] is to calculate the cross section of each state in terms of the quarkonium wave functions at the origin, that give the coupling of a quarkonium state to gluons and quarks. Given an interquark potential, the absolute cross section for each state is then unambiguously determined. It is this latter approach we will adopt in this paper.

We consider the production of η, ψ, and $\chi_{0,2}$ in the lowest order of α_s for each state. The contributing diagrams are shown in Fig. 5. Higher-order contributions including the one-loop virtual corrections to Fig. 5 lead to divergences which factorize as nonscaling effects in the parton distribution and a finite part which gives a multiplicative K factor by which the lowest-order cross section is corrected. These higher-order contributions have not been fully studied for the quarkonium production and so we take $K=1$ in this paper.

The cross section for quarkonium production by two-gluon fusion in pp collisions can be written in terms of the gluonic decay widths [(2.7), (2.9), and (2.10)] and the gluon distribution $g(x,Q^2)$ in a proton as[15]

$$\sigma(pp\to gg\to\mathcal{O}) = \frac{\pi^2\tau}{8M_{\mathcal{O}}{}^3}(2J+1)\Gamma(\mathcal{O}\to gg)\int_\tau^1 \frac{dx}{x} g(x,Q^2)g\left[\frac{\tau}{x},Q^2\right] \tag{3.1}$$

with $\tau=M_{\mathcal{O}}{}^2/s$ and J the spin of the quarkonium. Throughout we use the parton distributions[16] of Duke and Owens (set I) with $Q^2=m_Q{}^2$. The Eichten *et al.* parton distributions[17] give broadly similar results. We now turn to a discussion of the production rates for η, ψ, χ_0, and χ_2 quarkonia.

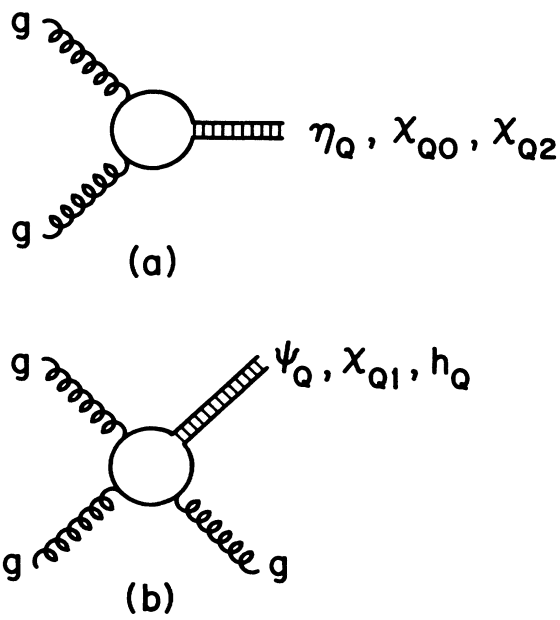

FIG. 5. Feynman diagrams for the production of the S- and P-wave quarkonium states by gluon collisions.

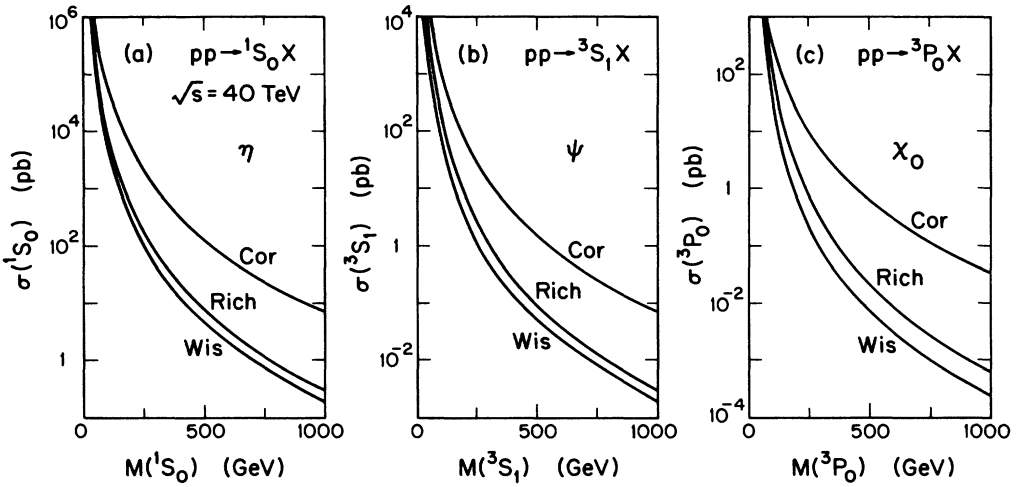

FIG. 6. The cross section for production of the η, ψ, and χ_0 states of heavy quarkonia as a function of the quarkonium mass in pp collisions at $\sqrt{s} = 40$ TeV. The cross section for χ_2 production is $\frac{4}{3}$ times that for χ_0 production. The three curves correspond to the cross sections obtained from the Cornell, Richardson, and Wisconsin potentials.

A. η production

The cross section for inclusive η production is shown in Fig. 6(a). The Cornell potential yields a cross section that exceeds the cross section obtained using the other potentials by a factor of over 20. The Coulomb, Richardson, and Wisconsin potentials give similar results that are probably more indicative of the true cross section. Even for η masses as large as 700 GeV and for the most conservative potential the cross section at $\sqrt{s} = 40$ TeV is ~ 1 pb, which corresponds to 10^4 events/yr for the SSC design luminosity.

B. ψ production

Color conservation together with Yang's theorem prevents the color singlet ψ from decaying into two gluons and so the lowest-order process is that shown in Fig. 5(b), the so-called bleaching gluon process. The cross section for the subprocess $gg \to \psi g$ is given by[1,3]

$$\hat{\sigma}(gg \to \psi g) = \frac{9\pi^2}{8M_\psi{}^3(\pi^2 - 9)} \Gamma(\psi \to ggg) I(\hat{s}/M_\psi{}^2) , \quad (3.2)$$

where

$$I(x) = \frac{2}{x^2}\left[\frac{x+1}{x-1} - \frac{2x \ln x}{(x-1)^2}\right] + \frac{2(x-1)}{x(x+1)^2} + \frac{4 \ln x}{(x+1)^3} . \quad (3.3)$$

There is no singularity as $x \to 1$ and one can integrate $\hat{\sigma}$ folded with gluon densities over $\hat{s}$ to obtain the total cross section. Figure 6(b) shows the ψ production cross section in pp collisions at $\sqrt{s} = 40$ TeV. Again there is a wide variation in the cross section obtained from the different potential models. The ψ cross section is roughly 2 orders of magnitude below that for η.

C. $\chi_{0,2}$ production

χ_0 and χ_2 quarkonia can be produced via two-gluon fusion, and so their production cross section can also be readily calculated using Eq. (3.1). The resulting cross section for χ_0 production is shown in Fig. 6(c). The corresponding cross section for χ_2 is $\frac{4}{3}$ times the χ_0 cross section. We note that since the χ cross sections are one order of magnitude smaller than the ψ cross sections and 3 orders of magnitude smaller than the η cross sections they are unlikely to be interesting.

D. Comments

We have ignored the following contributions to ψ production.

(a) Radiative χ decay, $\chi \to \psi\gamma$. The χ cross sections are an order of magnitude less than the ψ cross section, so even if the χ decayed radiatively 100% of the time, the contribution to the ψ cross section is a small effect compared to the uncertainty of the potential.

(b) Quark-antiquark annihilation, $q\bar{q} \to \psi$. Unless $M_\psi \simeq M_Z$, $\Gamma(\psi \to ggg) \sim \Gamma(\psi \to u\bar{u}) \sim \Gamma(\psi \to d\bar{d})$. Since the gg luminosity is much larger than the $u\bar{u}$, $d\bar{d}$ luminosities we expect the $q\bar{q} \to \psi$ contribution to the cross section to be negligible.

(c) WW fusion, $WW \to \psi$. As shown in Sec. IV, there is a large enhancement for the decay $\psi \to W^+W^-$. As a result, the WW fusion cross section $\hat{\sigma}(WW \to \psi)$ exceeds the bleaching gluon cross section by several orders of magnitude. However, the $W_L W_L$ luminosity[18] at the SSC is a million times smaller than the gluon luminosity and so this contribution can be neglected.

Finally we have neglected χ_1 and h production. These states cannot couple to two gluons and their decay widths are therefore $O(\alpha_s{}^3)$. The corresponding cross sections are then much smaller than those for $\chi_{0,2}$.

IV. DECAY MODES OF SUPERHEAVY QUARKONIA

In this section we present formulas for the decay widths of the S- and P-wave states of superheavy quarkonia.

The novel feature for quarkonia of mass $\gtrsim 200$ GeV is the appearance of new decay modes involving weak bosons and Higgs bosons. The coupling of the Higgs boson to a superheavy sequential quark, being proportional to the quark mass, exceeds the gauge couplings when $M > 2M_W$. Couplings of longitudinally polarized weak bosons are also effectively enhanced because the helicity-zero polarization vector of a gauge boson is proportional to E/M. There is no gauge-theoretical cancellation of the singular terms unlike the high-energy behavior of, say, WW scattering amplitudes, because a heavy fermion is involved here. Another way of seeing this enhancement is to recall that the longitudinal component of the weak boson comes from the unphysical Goldstone mode of the Higgs-boson field, which couples to the heavy quark with a large Yukawa coupling. Thus the decays of heavy quarkonia into W^+W^-, ZZ, $Z\gamma$, and also ZH and HH may be enhanced relative to the gluonic decay mode. In some cases these modes indeed dominate the quarkonium decay.

These annihilation decays do not exhaust all the possible decay modes of a superheavy-quarkonium state. Radiative and hadronic cascade decays to lower-mass states are possible except for the lowest pseudoscalar state. However, it turns out that these transitions are negligible for the S-wave states and at most of the same order as the annihilation decays for the P-wave states.

A potentially important decay mode is the single-quark decay; the quark or the antiquark decays weakly, leaving the other as a spectator. As is well known, the weak decay becomes increasingly important as the quark mass increases, proportional to $m_Q{}^5$ below the W emission threshold, or to $m_Q{}^3$ if the real W emission is allowed. In fact, if the t quark is very heavy ($\gtrsim M_W$), this single-quark decay becomes the dominant decay mode of the t-quarkonium states and hides all the other interesting modes. However, for the lower-mass member of the fourth-generation quark doublets, we expect that the single-quark decay is suppressed by the small intergeneration mixing. Some aspects of heavy-quarkonia decay have also been considered in Ref. 12.

A. Single weak decay

The width of an arbitrary quarkonium state $\mathcal{O}(Q\bar{Q})$ due to $Q \to q + W$ is[19,20]

$$\Gamma(\mathcal{O} \to Q\bar{q}W \text{ or } \bar{Q}qW) = \frac{\alpha_W |U_{Qq}|^2 \tilde{\beta}}{8} \frac{M_Q{}^3}{M_W{}^2} \times [1 + 4(R_W - 2R_q) + 16(R_q{}^2 + R_q R_W - 2R_W{}^2)] , \tag{4.1}$$

where U_{Qq} is the quark mixing matrix element, $\alpha_W = \alpha/\sin^2\theta_W$, $R_i = M_i{}^2/M^2$ for $i = W,q$. M is the quarkonium mass and

$$\tilde{\beta} = [1 - 8(R_q + R_W) + 16(R_q - R_W)^2]^{1/2} . \tag{4.2}$$

The width in Eq. (4.1) divided by $|U_{Qq}|^2$ is plotted in Fig. 7, for the cases $m_q = 0$ and $m_q = m_t = 40$ GeV. If there is no suppression due to the mixing, as would be the case for the heavy t quark or the heavier member of the fourth-generation quark doublet, the single-quark decay width is huge, exceeding 1 GeV at $M_{\mathcal{O}} \gtrsim 250$ GeV and ~ 10 GeV for $M_{\mathcal{O}} \sim 500$ GeV. Then the branching fractions to the decay modes of interest become insignificant.

The situation may be radically different for the lighter member of the doublet. From our experience with the known quarks, it appears that the intergeneration mixing becomes smaller for heavier quarks. Most of the speculations[20,21] on four-generation mixing suggest a small ($\lesssim 10^{-2}$) mixing of the fourth-generation quark to lighter quarks. If the mixing is 10^{-2}, the single-quark decay is suppressed by a factor of 10^4. Figure 7 shows that the weak decay width in this case is 100 keV—4 Mev for quarkonium of mass 250—800 GeV, which is smaller than the two-gluon decay width of the pseudoscalar state. Thus the single weak decay can be plausibly be neglected for the η quarkonium if the mixing is less than 10^{-2}. [We will subsequently see (Fig. 13) that a similar situation occurs for the ψ also.] We will make this assumption, particularly when we discuss quarkonium signatures at the SSC. The mixing must even be smaller if we require that the decay of the P-wave states should also be dominated by annihilation channels. It may well be that only the S-wave states of heavy quarkonium that decay dominantly via $Q\bar{Q}$ annihilation.

We note here that in any two-Higgs-doublet model

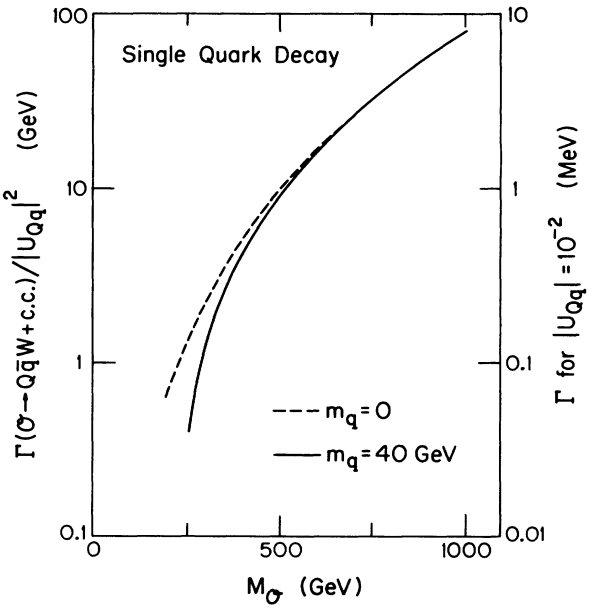

FIG. 7. The decay width of heavy quarkonium via the weak decay of a single quark divided by the square of the quark mixing matrix element squared. Also shown is the width for $|U_{Qq}| = 10^{-2}$.

without flavor-changing neutral currents (e.g., all supersymmetric models), single-charged-Higgs-boson emission provides a new possibility for single-quark decay of a heavy quark. However, the rate for this is suppressed by the same mixing-angle factor discussed above.

It is worth noting that the up and down quarks of a heavy SU(2) doublet are approximately degenerate in models where their masses are determined by the infrared fixed points of the equations governing the renormalization-group evolution of their Yukawa couplings from the unification scale down to low energies.[22] In this case, the decay of even the heavier member of the doublet is kinematically suppressed so that the considerations of this paper may be applicable to both the up- and down-type quarkonia.

B. Annihilation decays

Here we present the decay widths of all the S- and P-wave quarkonium states to two-body final states within the standard model. A substantial part of the results have not appeared in literature.[23] Formulas are given for fourth-generation quarkonium states, but they are also applicable to states made of quarks with unconventional quantum numbers (for instance, the isosinglet quarks in E_6 models) unless otherwise noted. The formulas require modification if the couplings to Higgs bosons differ from the standard-model coupling.

Each formula has been derived using two different calculational techniques, which provides a check of the computation. The first method developed in Ref. 14 involves writing the spin-projected amplitude near the threshold as a trace of a product of Dirac matrices; this amplitude can be readily squared to obtain the decay rates. The other technique is a direct derivation from the scattering amplitudes for states with definite helicity. The formalism for both methods is explained in Appendix A and illustrated explicitly for the decays $\mathcal{O}\to ZZ$ in Appendix B.

QCD corrections[24] to some of the decay modes have been calculated, and it is found that not all of them are small for charmonium and b-quarkonium systems. We have ignored these corrections because (a) higher-order calculations are available for only some of the decay modes and (b) the corrections are expected to be smaller for the heavy quarkonium.

In the following, each final state is discussed separately for all the S-wave ($\eta_Q:0^{-+},\psi_Q:1^{--}$) and P-wave ($\chi_{QJ}:J^{++},J=0,1,2,h_Q:1^{+-}$) quarkonia for convenience of presentation. The branching fractions for the various states will be given later in this section.

1. $\gamma\gamma$, gg, ggg

Widths for the decays to two massless vector states are well known but we reproduce them here for completeness. Yang's theorem forbids the decay of spin-1 states to two massless identical spin-1 particles; thus the ψ,χ_1,h states cannot decay into $\gamma\gamma$ or gg. (Yang's theorem is applicable for the two-gluon state since the initial state is a color singlet.) The generic diagrams responsible for the decays of all the quarkonia are shown in Fig. 8. Those contributing to the various decays of the quarkonium states can be read from Table I. For example, for the decay $\eta\to\gamma\gamma$, only the t- and u-channel quark-exchange graphs in Figs. 8(d) and 8(e) contribute. The decay widths to two photons are

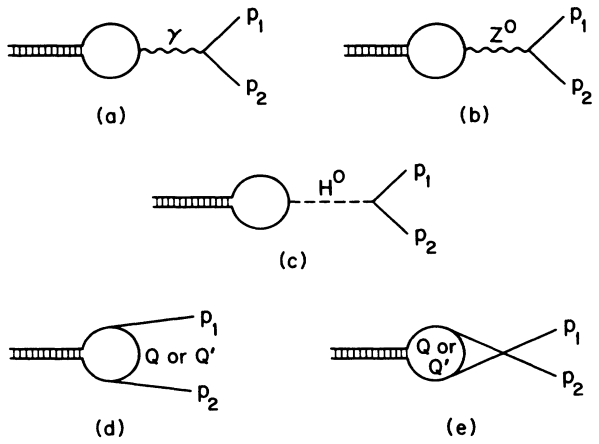

FIG. 8. Generic diagrams for the decay $\mathcal{O}_Q\to p_1p_2$ where p_1p_2 are gauge-boson pairs, fermion-antifermion pairs, a gauge-boson—Higgs-boson pair, or a Higgs-boson pair, and $\mathcal{O}_Q$ is the quarkonium. (a), (b), and (c) denote decays via the exchange of γ, Z^0, or H in the s channel while (d) and (e) denote decays via a quark exchange in the t or u channel. For $\mathcal{O}_Q\to W^+W^-$, the exchanged quark is the SU(2) partner (Q') of the quark contained in the quarkonium. The diagrams relevant for each decay mode discussed in Sec. IV can be read off from Table I.

$$\Gamma(\eta\to\gamma\gamma)=\frac{12\alpha^2e_Q{}^4}{M^2}\,|R_S(0)|^2\,, \tag{4.3}$$

$$\Gamma(\chi_0\to\gamma\gamma)=\frac{432\alpha^2e_Q{}^4}{M^4}\,|R'_P(0)|^2\,, \tag{4.4}$$

$$\Gamma(\chi_2\to\gamma\gamma)=\frac{576\alpha^2e_Q{}^4}{5M^4}\,|R'_P(0)|^2\,, \tag{4.5}$$

where we have omitted the suffix Q on the states for clarity. M is the mass of the quarkonium, e_Q is the charge of the quark Q in units of the proton charge.

The decay widths of the η, ψ, χ_0, and χ_2 states into gluons have already been given in Sec. II. In addition to these, the χ_1 and h states can also decay via $\mathcal{O}\to q\bar{q}g$ or ggg. The widths for these states have a singularity when the binding energy is neglected. These widths are $O(\alpha_s{}^3\ln\alpha_s)$ for heavy quarkonia and have been discussed in Ref. 9.

2. $f\bar{f}$

From Table I we see that quarkonium states can decay into a lighter fermion-antifermion pair via s-channel γ, Z, or Higgs-boson exchange, or via t-channel W exchange. First we note that the W exchange can be neglected since for the decay

TABLE I. The diagrams contributing to the allowed two-body decays $\mathcal{O}_Q \to p_1 p_2$ for the S- and P-wave quarkonium states. The entries (a—e) in the table refer to the five generic diagrams shown in Fig. 8.

p_1p_2 \ $\mathcal{O}_Q$	η_Q	ψ_Q	χ_{Q0}	χ_{Q1}	χ_{Q2}	h_Q
$\gamma\gamma$	d,e		d,e		d,e	
$f\bar{f}$	b	a,b	c	b		
$Z^0\gamma$	d,e	d,e	d,e	d,e	d,e	d,e
Z^0Z^0	d,e	d,e	c,d,e	d,e	d,e	d,e
W^+W^-	d	a,b,d	c,d	b,d	d	d
ZH	b	b,d,e		b,d,e	d,e	d,e
γH		d,e				d,e
HH			c,d,e		d,e	

$$(Q\bar{Q}) \to q\bar{q} \quad (e_Q \neq e_q) , \tag{4.6}$$

the interference term of the W exchange and other diagrams is suppressed by $|U_{Qq}|^2$. This interference contribution, though formally of the same order $|U_{Qq}|^2$ as the single weak decay [Eq. (4.1)], is further suppressed by the wave function at the origin factor that occurs only for the decay via annihilation. The potentially interesting flavor-changing decay $(Q\bar{Q}) \to Q'\bar{q}$, where $m_{Q'} > m_Q$, is also suppressed by the same factor. We will, therefore, neglect the W graph from now on.

Initial states which decay to $f\bar{f}$ (f denotes a quark or a lepton) is restricted since the diagrams are all s-channel exchange. The photon exchange contributes only to the 1^{--} quarkonium state, Higgs-boson exchange to 0^{++}, the Z exchange to 1^{--} (via vector coupling) and $0^{-+}, 1^{++}$ (via axial-vector coupling). The other two states, χ_2 and h, do not decay to $f\bar{f}$. Also, decays of η, χ_0 to a massless fermion pair are forbidden by chirality conservation.

The nonzero partial widths for the decays to $f\bar{f}$ with a finite fermion mass are listed below:

$$\Gamma(\eta \to f\bar{f}) = \frac{3\alpha_Z^2 N_f \beta_f}{32} \frac{M_f^2}{M_Z^4} |R_S(0)|^2 , \tag{4.7}$$

$$\Gamma(\psi \to f\bar{f}) = \frac{4\alpha^2 N_f \beta_f}{M^2} \left[(1+2R_f) \left[e_Q^2 e_f^2 + \frac{2e_Q e_f v_Q v_f}{x_W(1-x_W)} \frac{1}{1-R_Z} + \frac{v_Q^2 v_f^2}{x_W^2(1-x_W)^2} \frac{1}{(1-R_Z)^2} \right] + \beta_f^2 \frac{v_Q^2 a_f^2}{x_W^2(1-x_W)^2} \frac{1}{(1-R_Z)^2} \right] |R_S(0)|^2 , \tag{4.8}$$

$$\Gamma(\chi_0 \to f\bar{f}) = \frac{27\alpha_z^2 N_f \beta_f^3}{8} \frac{M_f^2}{M^2 M_Z^4} \frac{1}{(1-R_H)^2} |R'_P(0)|^2 , \tag{4.9}$$

$$\Gamma(\chi_1 \to f\bar{f}) = \frac{96\alpha_Z^2 a_Q^2 N_f \beta_f}{M^4} \frac{1}{(1-R_Z)^2} [v_f^2(1+2R_f) + a_f^2 \beta_f^2] |R'_P(0)|^2 . \tag{4.10}$$

Here, $\alpha_Z = \alpha/(\sin^2\theta_W \cos^2\theta_W)$, N_f is a color factor (1 for leptons, 3 for quarks), $R_i = M_i^2/M^2$ $(i = f, Z, H)$, $x_W = \sin^2\theta_W$, $\beta_f = (1-4R_f)^{1/2}$ is the velocity of the final fermion in the quarkonium rest frame, and v_i and a_i, the vector and axial-vector coupling of the fermion $i = f$ or Q to the Z^0, are given by

$$v_i = \tfrac{1}{2}(I_{3L} + I_{3R}) - e_i \sin^2\theta_W , \quad a_i = \tfrac{1}{2}(I_{3L} - I_{3R}) . \tag{4.11}$$

Here, I_{3L} (I_{3R}) is the third component of the weak isospin for the left- (right-) handed fermion. For sequential fermions $I_{3L} = \pm\frac{1}{2}$, $I_{3R} = 0$. The formula (4.8) for the ψ is standard; the χ_1 width (4.10) to massless fermion has been calculated by Kaplan and Kühn.[25] The above formulas are also applicable to decays of quarkonia formed from isosinglet quarks, except for the χ_0 result which involves Higgs-boson exchange. The singularity in Eqs. (4.8)—(4.10) is an artifact of the zero width approximation for Z^0 and H and can be simply treated by including the width into the respective propagators.

3. $Z\gamma$

The decay to a Z^0 and a photon is accessible when the quarkonium is heavier than M_Z. The diagrams are the same as those for $\gamma\gamma$, with one γ replaced by Z^0. All six quarkonium states can decay into $Z\gamma$. The decay widths may be obtained by crossing from the results for

$Z\to\gamma+$quarkonium of Guberina *et al.*[14] and also appear in Ref. 23. We have checked the results by independent calculations. The $Z\gamma$ decay rates are given by

$$\Gamma(\eta\to Z\gamma)=\frac{24\alpha\alpha_Z e_Q{}^2 v_Q{}^2}{M^2}(1-R_Z)\,|R_S(0)|^2\,, \tag{4.12}$$

$$\Gamma(\psi\to Z\gamma)=\frac{8\alpha\alpha_Z e_Q{}^2 a_Q{}^2}{M_Z{}^2}(1-R_Z{}^2)\,|R_S(0)|^2\,, \tag{4.13}$$

$$\Gamma(h\to Z\gamma)=\frac{96\alpha\alpha_Z e_Q{}^2 a_Q{}^2}{M_Z{}^2M^2}(1-R_Z{}^2)\,|R'_P(0)|^2\,, \tag{4.14}$$

$$\Gamma(\chi_0\to Z\gamma)=\frac{864\alpha\alpha_Z e_Q{}^2 v_Q{}^2}{M^4}\,\frac{(1-\frac{1}{3}R_Z)^2}{1-R_Z}\,|R'_P(0)|^2\,, \tag{4.15}$$

$$\Gamma(\chi_1\to Z\gamma)=\frac{192\alpha\alpha_Z e_Q{}^2 v_Q{}^2}{M^4}\,\frac{R_Z(1+R_Z)}{1-R_Z}\,|R'_P(0)|^2\,, \tag{4.16}$$

$$\Gamma(\chi_2\to Z\gamma)=\frac{1152\alpha\alpha_Z e_Q{}^2 v_Q{}^2}{5M^4}\,\frac{1+\frac{1}{2}R_Z+\frac{1}{6}R_Z{}^2}{1-R_Z}\,|R'_P(0)|^2\,. \tag{4.17}$$

The apparent singularity for $M_Z=M_\chi$ for the decays $\chi_J\to Z\gamma$ for $M_Z=M_\chi$ is due to our neglect of the binding energy for the quarkonia. The decay of the charge-conjugation-even states (η,χ's) proceeds by the vector coupling of the Z, that of C-odd states (ψ,h) by the axial-vector coupling. These latter widths are singular in the limit $M_Z\to 0$. This shows the nondecoupling of the longitudinal Z polarization, due to nonconservation of the axial-vector current. Further, the widths for $\psi,h\to Z_T+\gamma$ ($Z_T=$transversely polarized Z) are also nonvanishing in this limit since Yang's theorem is not applicable. (The $\chi_1\to Z\gamma$ width, on the other hand, vanishes in the same limit.) These properties can be translated to the case $M\to\infty$, i.e., the case of very heavy quarkonia, because the $M_Z\to 0$ and $M\to\infty$ limits are essentially equivalent. The $Z\gamma$ width of the C-even states has a regular behavior and becomes proportional to the $\gamma\gamma$ and gg width (except for χ_1), whereas, the width of the C-odd states has an enhancement factor which reflects the singular behavior in the $M_Z\to 0$ limit. For example, we can see that

$$\frac{\Gamma(\psi\to Z\gamma)}{\Gamma(\psi\to f\bar{f})}\propto\frac{M^2}{M_Z{}^2}\,.$$

The decay to the massive gauge boson becomes increasingly more important for a heavier-quarkonium state. Another way of understanding this enhancement is the following. The behavior comes from the longitudinally polarized Z^0, the spin vector being proportional to M/M_Z, and is thus the first example of the enhancement mentioned at the beginning of this section. Why is there no enhancement factor in the decay widths of the η and χ's, which are due to the vector coupling? This is because the vector current is conserved. At high energies, the longitudinal-polarization vector of a Z^0 with four-momentum k^μ is

$$\epsilon^\mu=\frac{1}{M_Z}k^\mu+O\left[\frac{M_Z}{k^0}\right]\,.$$

The first term, which may given an enhancement factor, does not contribute to the amplitude because of current conservation.

4. ZZ

It is convenient to begin with the discussion of possible quantum numbers of the ZZ system. We assign $J^{PC}=1^{--}$ to Z^0, $J^P=1^-$ to $W^\pm$, $J^{PC}=0^{++}$ to the Higgs boson. The gauge-Higgs system then conserves the symmetries C, P, and T separately. The fermion couplings to Z,W violates C and P, but within the range of considerations in this paper CP can be regarded as a good symmetry.

The total angular momentum of the ZZ system $\mathbf{J}$ is given by $\mathbf{J}=\mathbf{L}+\mathbf{S}$, where $\mathbf{L}$ is the orbital angular momentum between the two Z's, and S is the total spin ($S=0,1,2$). The parity and charge-conjugation quantum number of the system are given by $P=(-1)^L$, $C=(-1)^{L+S}$. Bose symmetry requires $L+S=$even; hence only $C=+$ states are allowed. Possible quantum numbers for low L states are listed in Table II. This table will be useful later in understanding the characteristic properties of various decay widths.

Possible states are much more restricted for the Z_LZ_L state, i.e., both Z's longitudinal. All $CP=-$ states are disallowed because in this case L and S are both odd and the $S=1$ spin wave function contains only Z_TZ_T. The Z_LZ_L component is also absent in J-odd, L-even states, which can be verified by using symmetry properties of the Clebsch-Gordan coefficients. Thus the only states decaying to Z_LZ_L are $0^{++},2^{++},\ldots$. This is in accord with the spectrum of two unphysical Goldstone-boson system.

The Feynman diagrams contributing to the ZZ decay are the t- and u-channel quark-exchange diagrams, which are common to the two-photon decay, and the s-channel Higgs-boson-exchange diagram (see Table I). The Higgs-boson diagram contributes only to the χ_0 decay. The decay widths are

TABLE II. Possible quantum numbers J^{PC} of the ZZ system for $L=0,1,2$.

J	$L=0$ $S=0,2$	$L=1$ $S=1$	$L=2$ $S=0,2$
0	0^{++}	0^{-+}	0^{++}
1		1^{-+}	1^{++}
2	2^{++}	2^{-+}	2^{++}
3			3^{++}
4			4^{++}

$$\Gamma(\eta\to ZZ)=\frac{12\alpha_Z{}^2(v^2+a^2)\beta_Z{}^3}{M^2}\frac{1}{(1-2R_Z)^2}\,|R_S(0)|^2\,, \tag{4.18}$$

$$\Gamma(\psi\to ZZ)=\frac{8\alpha_Z{}^2v^2a^2\beta_Z{}^5}{M_Z{}^2}\frac{1}{(1-2R_Z)^2}\,|R_S(0)|^2\,, \tag{4.19}$$

$$\Gamma(h\to ZZ)=\frac{96\alpha_Z{}^2v^2a^2\beta_Z{}^3}{M^2M_Z{}^2}\frac{1}{(1-2R_Z)^2}\,|R'_P(0)|^2\,, \tag{4.20}$$

$$\Gamma(\chi_0\to ZZ)=\frac{96\alpha_Z{}^2\beta_Z}{M_Z{}^4}\left[\left[v^2\frac{2R_Z{}^2}{(1-2R_Z)^2}-a^2+\frac{3}{32}\frac{1-2R_Z}{1-R_H}\right]^2+\frac{1}{2}R_Z{}^2\left[\frac{-v^2(3-8R_Z)+a^2(3-4R_Z)}{(1-2R_Z)^2}-\frac{3}{8}\frac{1}{1-R_H}\right]^2\right]|R'_P(0)|^2\,, \tag{4.21}$$

$$\Gamma(\chi_1\to ZZ)=\frac{48\alpha_Z{}^2\beta_Z{}^5}{M^2M_Z{}^2}\frac{1}{(1-2R_Z)^2}\left[a^2-v^2\frac{2R_Z}{1-2R_Z}\right]^2|R'_P(0)|^2\,, \tag{4.22}$$

$$\Gamma(\chi_2\to ZZ)=\frac{48\alpha_Z{}^2\beta_Z}{5M_Z{}^4}\left[\left[a^2+v^2\frac{4R_Z{}^2}{(1-2R_Z)^2}\right]^2+\frac{3R_Z}{(1-2R_Z)^2}\left[a^2+v^2\frac{2R_Z}{1-2R_Z}\right]^2+(v^2+a^2)^2\frac{4R_Z{}^2}{(1-2R_Z)^2}\left[3+\frac{2R_Z{}^2}{(1-2R_Z)^2}\right]\right]|R'_P(0)|^2\,, \tag{4.23}$$

where $\beta_Z=(1-4R_Z)^{1/2}$ and we have omitted here the subscript Q in v_Q and a_Q. In applying these formulas to unconventional quarkonia, the Higgs-boson contribution must be modified according to the model. Each of the six formulas (4.18)—(4.23) display large diversity.

(1) Parity. The amplitudes for ψ and h are parity violating (proportional to va), whereas those for η and χ's are parity conserving (proportional to v^2 or a^2). This property can be understood with the help of Table II. The quantum numbers of η and χ's ($J^{PC}=0^{-+},0^{++},1^{++},2^{++}$) can be found in Table II, but those of ψ and h ($1^{--},1^{+-}$) are not present therein. Thus the decay of these two states must proceed via the parity-violating coupling to $J^{PC}=1^{++},1^{-+}$ ZZ states, respectively.

(2) Threshold (β_Z) behavior. The χ_0 and χ_2 widths are proportional to β_Z, indicating that the final state can be in S wave. The η and h go into P wave, but the ψ and χ_1 widths, being D wave, are much suppressed at threshold ($M\gtrsim 2M_Z$). These different threshold behaviors follow from the orbital angular momentum L for each state as given in Table I. The width is proportional to $\beta_Z{}^{2L+1}$. For instance, the 0^{-+} state has $L=1$ and hence $\beta_Z{}^3$ behavior.

(3) High-mass ($M\to\infty$) limit. Because there are two Z's, the width can be enhanced by a factor $M^4/M_Z{}^4$ if both Z's are longitudinal. This double enhancement only occurs for χ_0 and χ_2, in accordance with our preceding discussion of the Z_LZ_L system. The other three states (ψ,h,χ_1) receive single enhancement only. There is no enhancement factor for the η because Z_LZ_T states cannot be in $J=0$.

Finally, the two-photon decay widths may be derived from the ZZ widths formula if we set $v=e_Q$, $a=0$, discard the Higgs-boson contribution ($R_H\to\infty$), and take the limit $R_Z\to 0$. The vector coupling is seen to give much milder heavy-mass dependence with no enhancement factor. Enhancement due to a heavy-quark mass is possible only if the axial-vector coupling is nonzero. From Eq. (4.11), this leads to the following: if the quark can have an SU(2)×U(1)-invariant mass term, there is no enhancement in the ZZ decay. This comment applies to isosinglet quarks, for example.

5. W^+W^-

The W^+W^- decays are quite similar to ZZ, but there are a few important differences. The quantum numbers of the W^+W^- system are tabulated in Table III. There are more states than the ZZ system, because here there is no Bose symmetry constraint. This leads to somewhat different properties of the W^+W^- widths, as will be shown shortly. Double longitudinal state $W_L^+W_L^-$ can form $J^{PC}=0^{++},1^{--},2^{++},\ldots$ only.

From Table I we see that there is only one (t-channel)

TABLE III. Possible quantum numbers J^{PC} of the W^+W^- system for $L=0,1,2$.

J	$L=0$ $S=0,1,2$	$L=1$ $S=1$	$L=1$ $S=0,2$	$L=2$ $S=1$	$L=2$ $S=0,2$
0	0^{++}	0^{-+}			0^{++}
1	1^{+-}	1^{-+}	1^{--}	1^{+-}	1^{++}
2	2^{++}	2^{-+}	2^{--}	2^{+-}	2^{++}
3			3^{--}	3^{+-}	3^{++}
4					4^{++}

quark-exchange diagram for the W^+W^- decay. Instead there are s-channel γ- and Z-exchange diagrams, in addition to the Higgs-boson exchange. These s-channel graphs contribute to limited states only: γ to 1^{--}, Z to $1^{--},1^{++}$, and H to 0^{++}. The quark-exchange graph which contributes to all states obviously depends on the mass of the other quark in the same weak doublet. The decay widths to W^+W^- are given below. Here we assume the standard $V-A$ coupling and neglect the intergeneration mixing, taking $U_{QQ'}=1$. We obtain

$$\Gamma(\eta\to W^+W^-)=\frac{3\alpha_W{}^2\beta_W{}^3}{8M^2}\frac{1}{(1-R)^2}\,|R_S(0)|^2\,, \tag{4.24}$$

$$\Gamma(\psi\to W^+W^-)=\frac{\alpha_W{}^2\beta_W{}^3}{64}\frac{M^2}{M_W{}^4}\left[\frac{1+20R_W+12R_W{}^2}{(1-R_Z)^2}(1-8cR_Z+16c^2R_Z{}^2)\right.$$
$$\left.-\frac{4R_W(5+6R_W)}{(1-R)(1-R_Z)}(1-4cR_Z)+\frac{4R_W(2-R_W)}{(1-R)^2}\right]|R_S(0)|^2\,, \tag{4.25}$$

$$\Gamma(h\to W^+W^-)=\frac{3\alpha_W{}^2\beta_W}{2M^2M_W{}^2}\frac{1}{(1-R)^2}\left[1-2R_W+R_W\left[1-\frac{\beta_W{}^2}{1-R}\right]^2\right]|R'_P(0)|^2\,, \tag{4.26}$$

$$\Gamma(\chi_0\to W^+W^-)=\frac{3\alpha_W{}^2\beta_W}{4M_W{}^4}\left\{\left[\frac{1}{1-R}\left[1-3R_W+\frac{\beta_W{}^2R_W}{1-R}\right]-\frac{3}{1-R_H}(\tfrac{1}{2}-R_W)\right]^2\right.$$
$$\left.+2R_W{}^2\left[\frac{1}{1-R}\left[1-\frac{\beta_W{}^2}{1-R}\right]-\frac{3}{1-R_H}\right]^2\right\}|R'_P(0)|^2\,, \tag{4.27}$$

$$\Gamma(\chi_1\to W^+W^-)=\frac{3\alpha_W{}^2\beta_W{}^3}{8M^2M_W{}^2}\frac{1}{(1-R)^2}\left[\frac{\beta_W{}^2(1-2R)^2}{(1-R)^2}+\left[\frac{\beta_W{}^2}{1-R}-\frac{4(R-R_Z)}{1-R_z}\right]^2\right.$$
$$\left.+\frac{R_W(R-R_Z)^2}{(1-R_Z)^2}\left[8+\frac{(1+2R_W)^2}{R_W{}^2}\right]\right]|R'_P(0)|^2\,, \tag{4.28}$$

$$\Gamma(\chi_2\to W^+W^-)=\frac{3\alpha_Q{}^3\beta_W}{40M_W{}^4}\frac{1}{(1-R)^2}\left[1+12R_W+56R_W{}^2-\frac{16\beta_W{}^2R_W(1+R_W)}{1-R}+\frac{6\beta_W{}^4R_W}{(1-R)^2}\right]|R'_P(0)|^2\,. \tag{4.29}$$

Here $\alpha_W=\alpha/\sin^2\theta_W$, $R=2(R_Q-R_{Q'}+R_W)$ (actually $R_Q=\frac{1}{4}$), $\beta_W=(1-4R_W)^{1/2}$, with $R_W=M_W{}^2/M^2$, and $c=2I_{3Q}e_Q\sin^2\theta_W$. It is straightforward to generalize the formulas to the case of finite mixing.

It is instructive to compare the W^+W^- formulas (4.24)—(4.29) with the ZZ widths (4.18)—(4.23). Half of the states (ψ,h,χ_1) have less suppressed W^+W^- threshold behavior due to the lack of Bose symmetry. Large-mass behavior is similar with a notable exception of ψ, which now gains a double enhancement. Thus for a very large mass quarkonia we have

$$\Gamma(\psi\to W^+W^-)\gg\Gamma(\psi\to ZZ)\,.$$

This is completely different from other states, for instance,

$$\Gamma(\chi_0\to W^+W^-):\Gamma(\chi_0\to ZZ)\approx 2:1\,,$$

which agree with naive expectation. The explanation of these behaviors can be made along a similar line of argument as was made for the ZZ system.

6. ZH

This decay can be enhanced due to the large Yukawa coupling of the heavy quark in addition to the longitudinal Z enhancement.

The ZH system is described by $\mathbf{J}=\mathbf{L}+\mathbf{S}$, $S=1$, $P=(-1)^{L+1}$, $C=-$, and is summarized in Table IV. All states except χ_0 can decay into ZH. The relevant dia-

TABLE IV. Possible quantum numbers J^{PC} of the ZH system for $L=0,1,2$.

J	$L=0$	$L=1$	$L=2$
0		0^{+-}	
1	1^{--}	1^{+-}	1^{--}
2		2^{+-}	2^{--}
3			3^{--}

grams can be read off from Table I. Graphs with t- or u-channel quark-exchange have a large Yukawa coupling. The s-channel Z-exchange graph does not have this coupling, but it has instead an enhancement coming from the longitudinal component of the Z propagator. Three states η, ψ, and χ_1 receive contribution from the Z-exchange graph.

The widths are[25]

$$\Gamma(\eta\to ZH)=\frac{3\alpha_Z{}^2 a_Q{}^2\beta_{ZH}{}^3}{4}\frac{M^2}{M_Z{}^4}\,|R_S(0)|^2\,, \tag{4.30}$$

$$\Gamma(\psi\to ZH)=\frac{\alpha_Z{}^2 v_Q{}^2\beta_{ZH}}{2M_Z{}^2}\frac{1}{(1-R_Z)^2(1-R_Z-R_Z)^2}\{[(1-R_Z)^2-R_H(1-3R_Z)]^2$$
$$+\tfrac{1}{2}R_Z[(1-R_Z)^2+R_H(2-R_H)]^2\}\,|R_S(0)|^2\,, \tag{4.31}$$

$$\Gamma(h\to ZH)=\frac{6\alpha_Z{}^2 v_Q{}^2\beta_{ZH}{}^3}{M^2 M_Z{}^2}\frac{1}{(1-R_Z-R_H)^2}\,|R_P'(0)|^2\,, \tag{4.32}$$

$$\Gamma(\chi_1\to ZH)=\frac{6\alpha_Z{}^2 a_Q{}^2\beta_{ZH}}{M_Z{}^4}\frac{1}{(1-R_Z-R_H)^2}\left\{(1+R_Z-R_H)^2\left[1-R_Z+\frac{R_H R_Z}{1-R_Z}\right]^2\right.$$
$$+\frac{1}{2}R_Z\left[3(1-R_Z)+R_H\right.$$
$$\left.\left.+4R_H R_Z\left[\frac{1}{1-R_Z}+\frac{1}{1-R_Z-R_H}\right]\right]^2\right\}|R_P'(0)|^2\,, \tag{4.33}$$

$$\Gamma(\chi_2\to ZH)=\frac{9\alpha_Z{}^2 a_Q{}^2\beta_{ZH}{}^5}{5M^2 M_Z{}^2}\frac{1}{(1-R_Z-R_H)^4}\,|R_P'(0)|^2\,, \tag{4.34}$$

where $\beta_{ZH}=[(1-R_Z-R_H)^2-4R_Z R_H]^{1/2}=2|\mathbf{q}|/M$, $\mathbf{q}$ being the three-momentum of the Z or H. These widths can be obtained by crossing from the results of Guberina *et al.*,[14] and can be found in Ref. 23. They have been independently checked by us.

It is interesting to compare those formulas with the $Z\gamma$ ones. The role of η and ψ is interchanged here: the $\eta\to ZH$ is doubly enhanced, whereas the ψ width has only one enhancement factor. The ZH widths of C-odd states come from the vector coupling, and so are only singly enhanced.

7. γH

Although the γH decay is similar to ZH, here there is no axial-vector coupling. Thus there is only one enhancement due to the Yukawa coupling and parity is conserved. C-even states η and χ's cannot decay into γH. The $\psi\to\gamma H$ decay was first discussed by Wilczek.[26] The partial width is

$$\Gamma(\psi\to\gamma H)=\frac{\alpha_W\alpha e_Q{}^2}{2M_W{}^2}(1-R_H)\,|R_S(0)|^2\,. \tag{4.35}$$

The other allowed γH decay has the width

$$\Gamma(h\to\gamma H)=\frac{6\alpha_W\alpha e_Q{}^2}{M^2 M_W{}^2}(1-R_H)\,|R_P'(0)|^2\,, \tag{4.36}$$

which was first derived by Kühn.[23]

8. HH

The two-Higgs-boson system has $J^{PC}=0^{++},2^{++},\ldots$ so this channel is not accessible from ψ, h, and χ_1 (angular momentum conservation) and from η (CP conservation). However, the two states χ_0 and χ_2 can decay into HH. There is a diagram with s-channel Higgs-boson exchange, which involves the three-Higgs-boson vertex and contributes to the χ_0 decay, apart from t- and u-channel quark-exchange graphs. Widths are doubly enhanced by the Yukawa coupling:

$$\Gamma(\chi_0\to HH)=\frac{3\alpha_W{}^2\beta_H}{32M_W{}^4}\left[\frac{5-8R_H}{(1-2R_H)^2}-\frac{9R_H}{1-R_H}\right]^2|R_P'(0)|^2\,, \tag{4.37}$$

$$\Gamma(\chi_2\to HH)=\frac{3\alpha_W{}^2\beta_H{}^5}{80M_W{}^4}\frac{1}{(1-2R_H)^4}\,|R_P'(0)|^2\,, \tag{4.38}$$

where $\beta_H=(1-4R_H)^{1/2}$. The second term of the χ_0 formula is the contribution of the three-Higgs-boson vertex. This completes the catalog of two-body annihilation decay rates for the S- and P-wave states of heavy quarkonium.

C. Radiative and hadronic transitions

A quarkonium state can make a transition to a lower-mass state by emitting a photon or light hadrons. Here we make an estimate of these transitions of the lowest S- and P-wave states. The only appreciable transition is the radiative decay of the P states.

1. S-wave states

The pseudoscalar state η is expected to have the lowest mass and is stable against cascade decay. The only possible transition of the ψ is the $M1$ transition $\psi\to\eta\gamma$ with a width

$$\Gamma(\psi\to\eta\gamma)=\frac{16\alpha e_Q{}^2k^3}{3M^2}\ , \tag{4.39}$$

where k is the photon energy $k\simeq M_\psi-M_\eta$. The $\psi-\eta$ mass difference comes from the spin-spin interaction

$$M_\psi-M_\eta\simeq\frac{32\alpha_s}{9M^2}\,|R_S(0)|^2=\frac{4}{3\alpha_s}\Gamma(\eta\to gg) \tag{4.40}$$

and is ~ 50 MeV for the Wisconsin potential. The width (4.39) is much smaller than 1 eV for the quarkonium mass range of interest and is completely negligible.

2. Radiative transitions of P-wave states

The P states χ_J,h can make $E1$ transition to the S states: $\chi_J\to\psi\gamma$, $h\to\eta\gamma$. (The $M1$ transition $\chi_2\to h\gamma$ is negligible.) The widths are[1]

$$\Gamma(\chi_J\to\psi\gamma)=\Gamma(h\to\eta\gamma)=\frac{4\alpha e_Q{}^2k^3}{9}\,|\langle S\,|\,r\,|\,P\rangle|^2\ . \tag{4.41}$$

The photon energy $k\simeq M_{1P}-M_{1S}$ is ~ 1 GeV and the radiative width (4.41) cannot be neglected. This fact may be understood from the following argument. For a power-law potential $V(r)\sim r^\nu$, the radiative width scales as[5]

$$\Gamma(\chi\to\psi\gamma)\sim m_Q^{-(2+3\nu)/(2+\nu)}\ , \tag{4.42}$$

when the quark mass is changed. The gluonic decay width scales as[5]

$$\Gamma(\chi\to gg)\sim m_Q^{-(3+4\nu)/(2+\nu)}\ . \tag{4.43}$$

The quark-antiquark potential may be effectively described by a power potential with $\nu\sim 0$ for the charmonium and b-quarkonium regions and with ν decreasing to -1 for very heavy quarkonium. The ratio

$$\frac{\Gamma(\chi\to\psi\gamma)}{\Gamma(\chi\to gg)}\sim m_Q^{(1+\nu)/(2+\nu)}$$

does not decrease as m_Q increases for $-1\le\nu\lesssim 0$. The P-wave radiative decay for the charmonium χ states has an appreciable branching fraction. Thus it should be also important for a heavier quarkonium.

Explicit calculation using the potentials shows that the radiative decay of a heavy P-wave states has a rate comparable to the gluonic decay $\chi_{0,2}\to gg$. The annihilation decay branching ratios are reduced due to this radiative mode as will be discussed later.

3. Hadronic transitions of P states

The P-wave states can also emit light hadrons to become an S state, for instance,

$$\chi_Q\to\eta_Q\pi\pi,\eta_Q\eta,\psi_Q\omega\ ,$$

$$h_Q\to\psi_Q\pi\pi,\ldots\ .$$

Since the size of the quarkonium states is much smaller than the extension of the light-hadron system, these decays can be evaluated by the QCD multipole expansion,[27] which describes the decays as

$$\chi_Q\to\eta_Q+gg,\ \text{etc.}$$

and is successful for the charmonium and b-quarkonium transition. These transitions account for a substantial part of the decay rate for states such as ψ',Υ'. However, the strong mass dependence of the widths makes them negligible for heavy-quarkonium states.

D. Branching fractions for quarkonium decay

We are now in a position to compute the branching fractions for the decays of S- and P-wave quarkonium states into the various two-body states discussed in Sec. IV B. For definiteness, we have presented our results for a down-type quarkonium. The branching fractions for the up-type quarkonium are somewhat different because of the different couplings to the photon and Z^0, but these can be readily calculated using the formulas in Sec. IV B. We first consider the case when the only allowed decays are into gauge boson or known fermion pairs. In this analysis, we assume $m_t=40$ GeV unless otherwise specified. The possibility that the Higgs boson or a fourth-generation charged lepton is light enough to be produced via quarkonium decay is deferred to Sec. IV D 2. Single-quark decay is ignored throughout.

1. Heavy-Higgs-boson case

(a) η decays. The branching fractions for the various possible decays of η are shown in Fig. 9. For η masses less than 1 TeV, the dominant decay is $\eta\to gg$ which proceeds via the strong interaction. For large η masses, the decay into a $t\bar{t}$ pair which occurs only due to axial-vector-current nonconservation starts to become important since it is enhanced by a factor $(M_\eta/M_Z)^4$ [see Eq. (4.7)] relative to the gluonic decay [Eq. (2.7)]. Thus for $m_t=100$ GeV, $\eta\to t\bar{t}$ dominates for $M_\eta>500$ GeV. For the same reason, decays of η into sequential heavy leptons may be important as we will subsequently see. There is, however, a suppression $(M_f/M_\eta)^2$ coming from the fact that the divergence of the axial-vector current is proportional to M_f. This cancels part of the enhancement just discussed.

Of particular interest are the rare but characteristic decays of the η into gauge-boson pairs: WW, ZZ, $Z\gamma$, and $\gamma\gamma$. Although the branching fraction for these is small, the large η-production cross section (see Fig. 6) leads to a fairly large number of gauge-boson pairs via η decay. However we find later that there are serious problems with backgrounds to these decay channels.

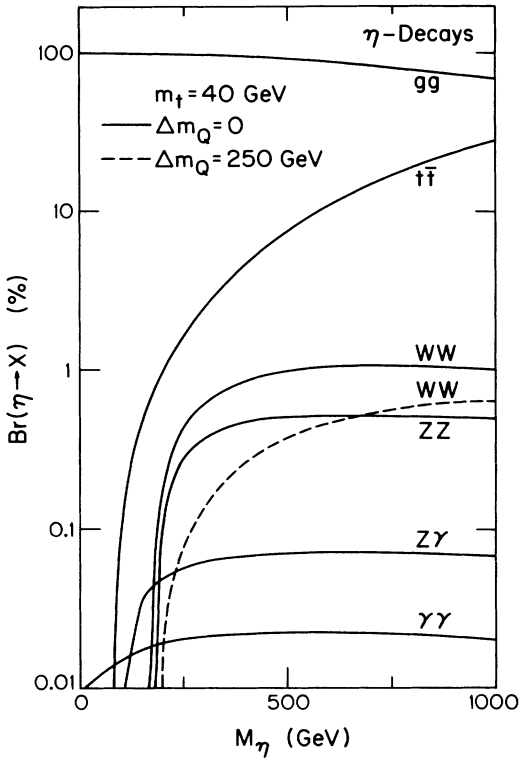

FIG. 9. The branching fraction for the decays of η_Q as a function of M_η. The W^+W^- branching fraction depends on the mass of Q' the SU(2) partner of Q and is shown for $m_{Q'}=m_Q$ (solid curve) and $m_{Q'}=m_Q+250$ GeV (dashed curve). Δm_Q in the figure denotes $m_{Q'}-m_Q$.

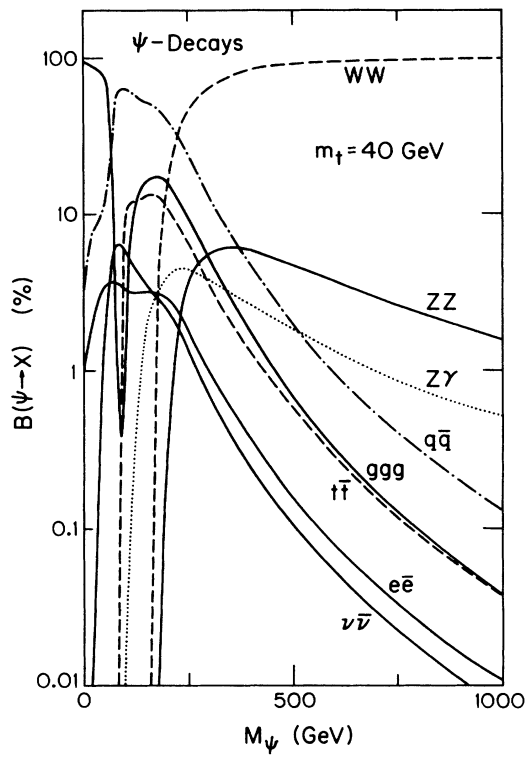

FIG. 10. The branching fractions for the decays of ψ_Q. We have fixed $m_{Q'}=m_Q+250$ GeV.

(b) ψ decays. The branching fractions for the allowed modes are shown in Fig. 10. Unlike the η case, the weak decays of ψ dominate the strong decay $\psi\to ggg$ for $M_\psi \gtrsim M_Z$. For $M_\psi=M_Z$, the decay $\psi\to Z\to f\bar{f}$ dominates ($f=q,l,\nu$) which accounts for the sharp dip in the branching fraction for $\psi\to ggg$ there. It is interesting to note that for $M_\psi > 2M_W$, the decay $\psi\to W^+W^-$ completely dominates all the other signals since it is the only "doubly enhanced" ψ decay, as discussed in Sec. IV B. The fact that the branching fraction for the W^+W^- mode is $\simeq 100\%$ implies that in spite of its much smaller production cross section, ψ decays compete with η decay as a source of W pairs.

(c) χ decays. The branching fractions for the various P-wave states are shown in Figs. 11(a)–11(c). The states χ_0 and χ_2 couple directly to two gluons so that the decays $\chi_{0,2}\to gg$ dominate until the doubly enhanced W^+W^- and Z^0Z^0 decays exceed the gluonic decays at $M_\chi \simeq 0.5$ TeV. The decays $Z\gamma$ and $\gamma\gamma$ have no enhancement factors, and, hence, their branching fractions are very small. Finally, the heavy-fermion decay of χ_0 is enhanced exactly as in the η case and hence is fairly small for $m_t=40$ GeV. The branching fractions shown do not add up to 100% because we have included the decays $\chi\to\psi\gamma$ (for the wave functions given by the Wisconsin potential) in the branching ratio. Since the matrix elements and the phase space for the transition are the same for the decay of all the χ states, the effect on the branching ratios is maximum for χ_1 since a light χ_1 is narrower than $\chi_{0,2}$ because it dominantly decays via $\chi_1\to q\bar{q}g$ (Ref. 9).

(d) h decays. Finally, we come to the decays of the singlet P-wave quarkonium state, for which the branching fractions are shown in Fig. 12. The decays $h\to W^+W^-$ and $h\to Z^0Z^0$ are only singly enhanced and hence the quarkonium mass for which these decays compete with the hadronic decays is somewhat larger than in the previous cases.

The total widths for the various quarkonium states are shown in Fig. 13. Also shown in the figure is the corresponding width from the single-quark decay assuming the mixing U_{Qq} between the third- and fourth-generation quarks is 0.01. We see that for $M_{\mathcal{O}} \gtrsim 230$ GeV, the single-quark decay dominates the annihilation decays for all the P-wave states. As discussed in Sec. IV A, the only quarkonium states amenable to the analysis in this paper are then the ψ and the η. If $U_{Qq} \lesssim 10^{-3}$, the single-quark decay mode becomes comparable to the annihilation decays even for the χ states.

2. *Quarkonium decays into Higgs bosons*

(a) Higgs-boson–γ decays. If the Higgs boson is lighter than $2m_Q$, the decay $\psi\to H\gamma$ can occur.[26] The C-

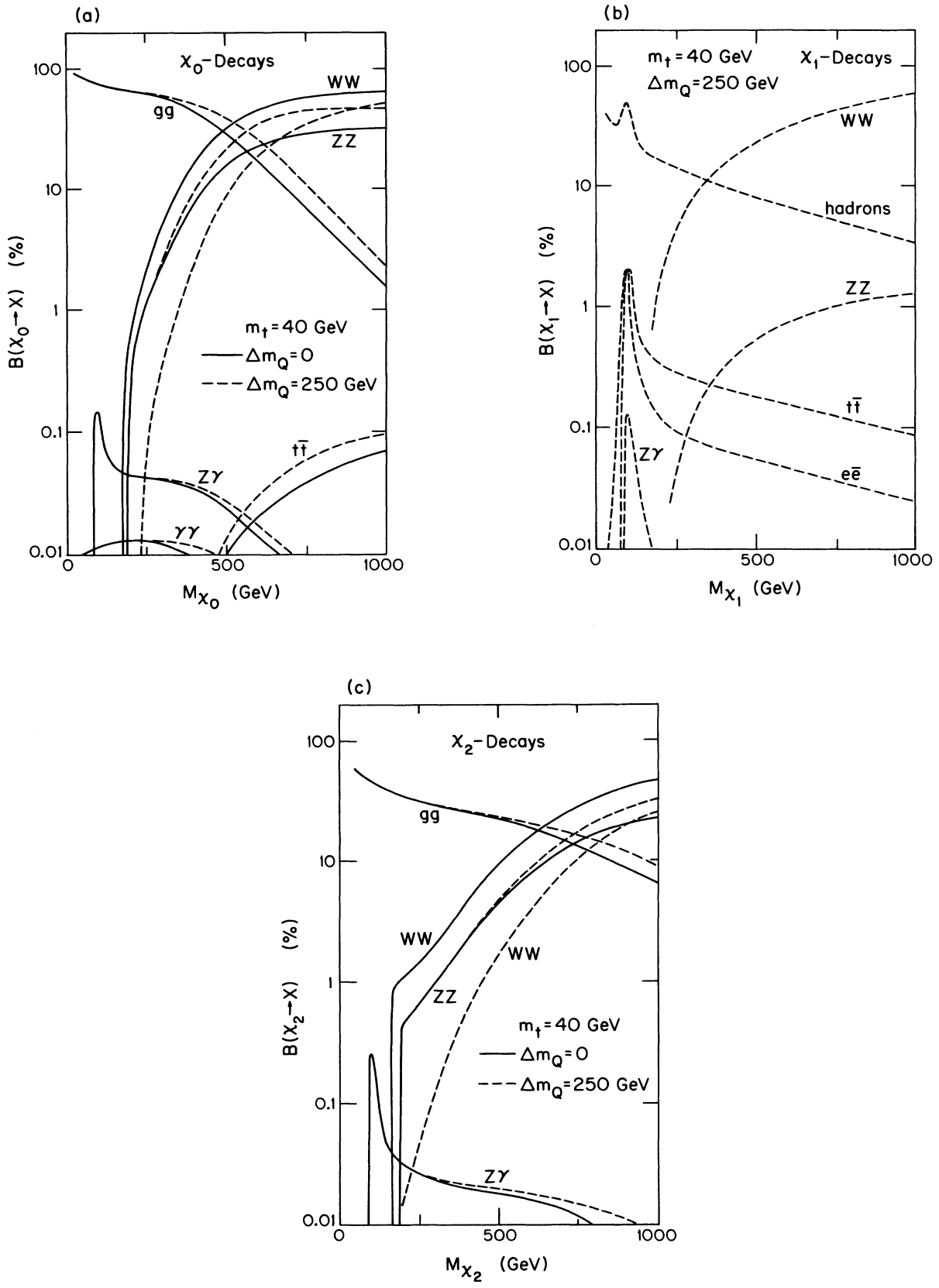

FIG. 11. The branching fractions for (a) χ_0 decays, (b) χ_1 decays, and (c) χ_2 decays as a function of the quarkonium mass.

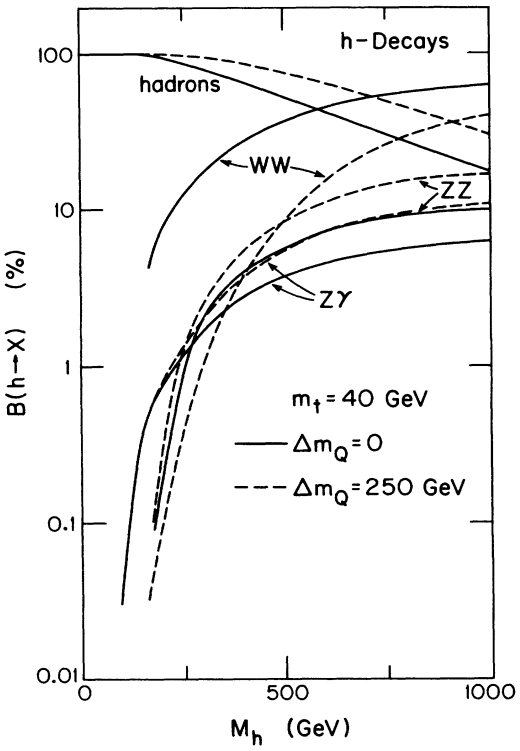

FIG. 12. The branching fraction for the decays of the $^1P_1$ quarkonium state h as a function of its mass.

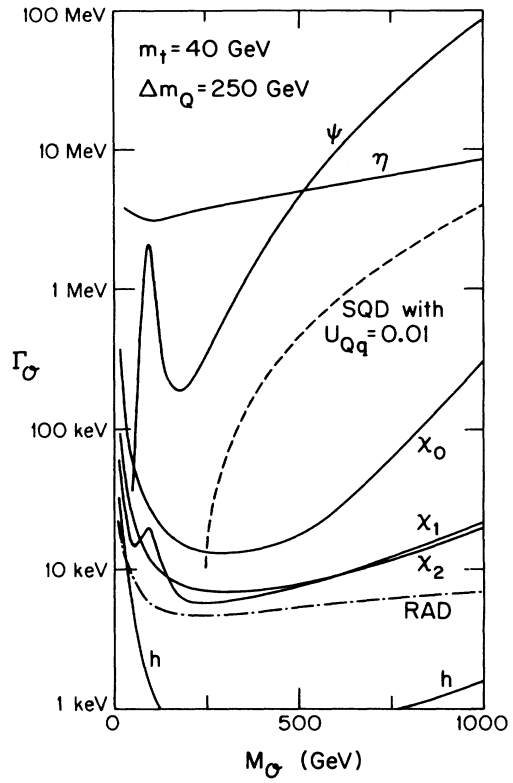

FIG. 13. A comparison of the total widths of the various S- and P-wave states resulting from the annihilation decays shown in Fig. 8 and Table I with the width resulting from the weak decay of the heavy quark assuming a mixing of 1%. In this case, the single-quark decay (SQD) rate shown by the dashed line exceeds the annihilation decay rate for P-wave states for quarkonium masses exceeding 250 GeV. Note that this rate varies as the square of the mixing matrix element U_{Qq}. In this figure we have assumed the Higgs boson is too heavy to be produced by the decay of quarkonium.

even states η and χ_J cannot decay via this mode leaving only the other possibility of $h\to H\gamma$. The $H\gamma$ branching fraction for the two states are shown in Fig. 14. Again the dip at $M_\psi = M_Z$ is due to $\psi\to Z\to f\bar{f}$; there is no corresponding dip for the h due to the fact that the fermion pair decay of h is forbidden. For a variety of Higgs-boson and quarkonium masses, this radiative decay mode is between 2% and $\gtrsim$15%. The signals from these decays could be potentially of interest at a high energy e^+e^- collider.

(b) Higgs-boson—Z^0 decays. Unlike the decay $\mathcal{O}\to H\gamma$, the C-even states (except for χ_0) can decay via $\mathcal{O}\to HZ^0$. Compared to the Wilczek process, the HZ^0 decay rate can be substantially enhanced for heavy quarkonium since the Z^0 can be longitudinally polarized. The branching fractions for the Z^0H decay of the various quarkonium states are shown in Fig. 15. If $M_\eta > 400$ GeV and $M_H \lesssim M_\eta - 250$ GeV, η dominantly decays via the Z^0H mode. The large production cross section for η together with this large branching for $\eta\to ZH$ leads to a possibly novel signature[2] for the intermediate-mass Higgs boson at the SSC, which will be discussed in the next section. Like the η, the decay $\chi_1\to ZH$ is also doubly enhanced. Unfortunately, χ_1 production is very small at the SSC, but this decay mode could potentially be of interest at a high-energy e^+e^- collider.

The decays of ψ and h into Z^0H are only singly enhanced as are the decays γH. The branching fractions for ψ and h into Z^0H are comparable to $H\gamma$ as shown in Fig. 14.

(c) Higgs-boson-pair decays. For heavy enough quarkonium masses, the states χ_0 and χ_2 can decay into Higgs-boson pairs with the branching fractions in Fig. 16. The decays of the other quarkonium states into this mode is forbidden by CP or angular momentum conservation. For a light enough Higgs boson, this is the dominant decay mode of the χ_0.

3. *Quarkonium decays into heavy leptons*

From our knowledge of the first three generations, it seems quite likely that a fourth-generation lepton (L) would be lighter than the fourth-generation quarks. Thus quarkonia could be a source of heavy-lepton pairs.

The branching fraction for the decay $\mathcal{O}\to L\bar{L}$ is shown in Fig. 17(a) for the case of a very heavy Higgs boson and in Fig. 17(b) for the case $m_H = 130$ GeV. We have nomi-

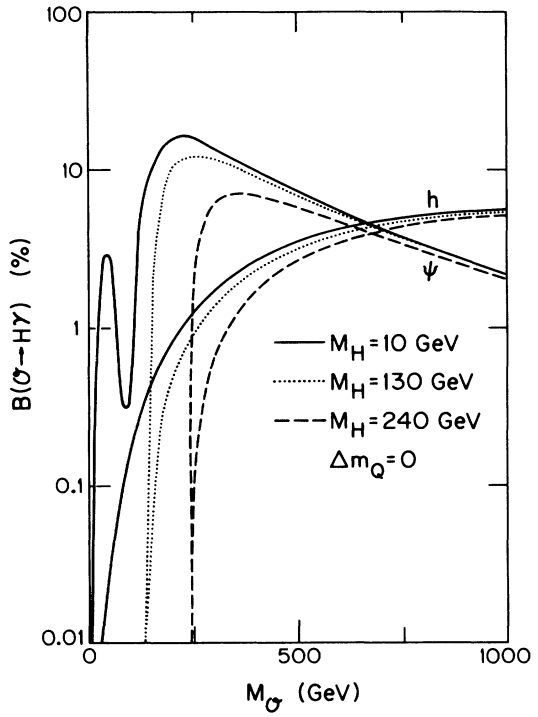

FIG. 14. The branching fractions for $\psi \to H\gamma$ and $h \to H\gamma$ decays vs the quarkonium mass for three different Higgs-boson masses.

nally chosen the heavy-lepton mass to be 100 GeV. The decay $\eta \to L\bar{L}$ has a substantial branching fraction (for the reasons noted in discussion of $\eta \to t\bar{t}$) unless the decay $\eta \to HZ^0$ is allowed. In the latter case the branching fraction for the HZ^0 mode increases rapidly with the heavy-quark mass and that for $\eta \to L\bar{L}$ reduces. It is also interesting to note that $\chi_0 \to L\bar{L}$ is allowed only via Higgs-boson exchange and hence this channel is important only for small M_H. The branching fraction for $\chi_0 \to L\bar{L}$ also falls off with increasing M_χ due to the dominance of the decay, $\chi_0 \to HH$.

This completes our discussion of the decays of heavy quarkonium. In the next section we turn to a study of the possible signals and backgrounds to the various decay modes studied here, in order to assess whether it is possible to identify new quarks at the SSC via quarkonium decays.

V. SUPERHEAVY-QUARKONIUM SIGNALS AT THE SSC

Fourth-generation quarkonium states are produced at sufficiently high rates to be observable at a high luminosity multi-TeV hadron collider such as the proposed SSC. This is particularly interesting since the anticipated luminosity ($\sim 10^4$ pb^{-1}/yr) may make it possible to search for relatively rare decay modes with distinctive signatures. A study of the various signals that result from quarkonium decays forms the subject of this section.

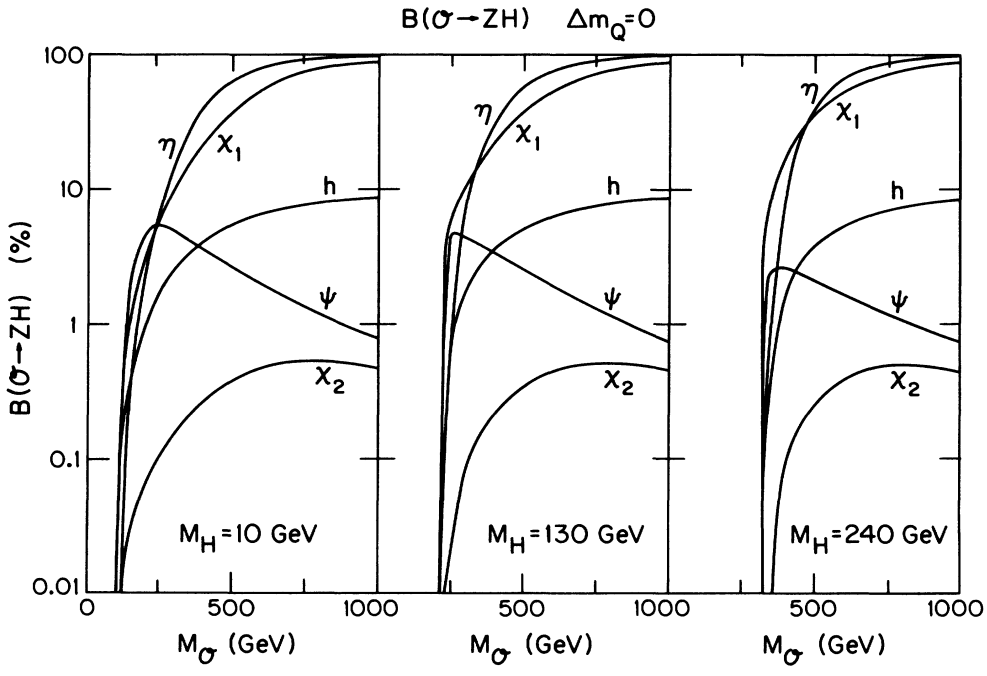

FIG. 15. The branching fractions for the ZH decay mode of heavy quarkonium vs the quarkonium mass for three different Higgs-boson masses. For definiteness $m_{Q'} = m_Q$ is assumed although the results are insensitive to this choice of Q' mass.

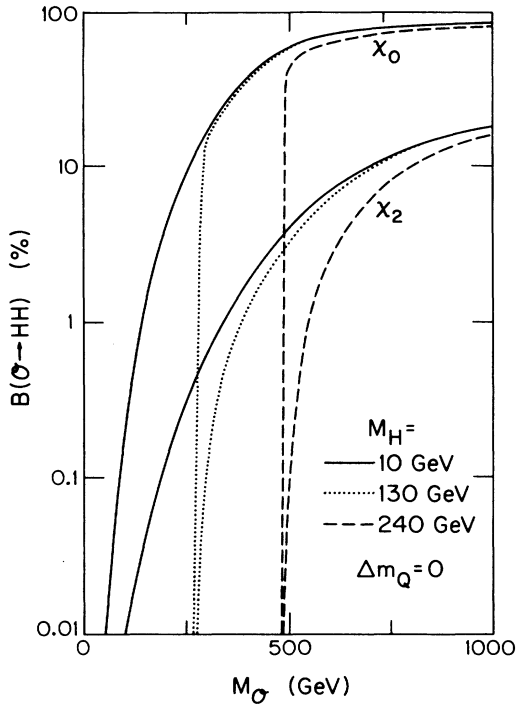

FIG. 16. The branching fractions for the decays $\chi_0 \to HH$ and $\chi_2 \to HH$ vs the quarkonium mass for three values of the Higgs-boson mass.

A. Heavy-Higgs-boson case: Quarkonium decays into gauge-boson and fermion pairs

Consider first the case where the Higgs boson and any new sequential leptons are too heavy to be produced via quarkonium decay. Ignoring the hadronic decays, which would be obscured by strong-interaction backgrounds, we are left with possible signals from gauge-boson pairs $\gamma\gamma$, $Z^0\gamma$, W^+W^-, and Z^0Z^0 and from lepton pairs l^+l^-. These modes would be characterized by a common invariant mass of the produced pair, and so the attainable mass resolution would be a crucial factor in deciding whether the quarkonium signal could be distinguished from backgrounds.

The total signals can be readily calculated from the quarkonium production rates in Sec. III and the branching fractions for various decay modes in Sec. IV. Our results for the various final states are shown in Fig. 18 for the case of a down-type quarkonium. The corresponding signals for the other potentials can be obtained by scaling those in Fig. 18 using Fig. 6. Most of the signal for neutral-gauge-boson pairs comes from η_Q because of its large production rate. The ψ_Q contributes most of the W^+W^- signal. The fact that the branching fraction for the decay $\psi \to W^+W^-$ is almost 100% compared with $<1\%$ for $\eta \to W^+W^-$ (see Fig. 10) makes up for the smallness of the ψ cross section relative to η. The lepton pairs dominantly come from ψ decay.

The reduction in the signal due to rapidity cuts in the

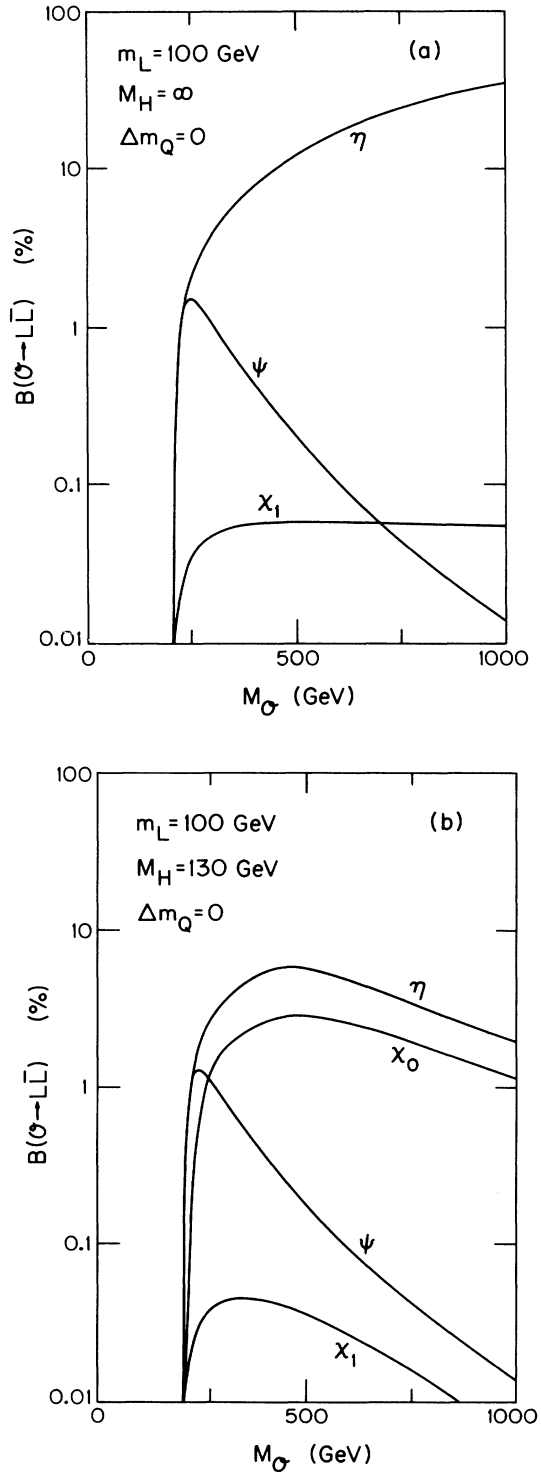

FIG. 17. The branching fraction for the decay $\mathcal{O} \to L\bar{L}$ assuming (a) that the Higgs boson is too heavy to be produced via $\mathcal{O}$ decay and (b) assuming $M_H = 130$ GeV. The presence of a relatively light Higgs boson affects the branching fractions for η and χ_1 since these have large branching fractions into ZH (Fig. 15) and also allows the channel $\chi_0 \to L\bar{L}$ to open up since this decay occurs only via s-channel Higgs-boson exchange (see Table I).

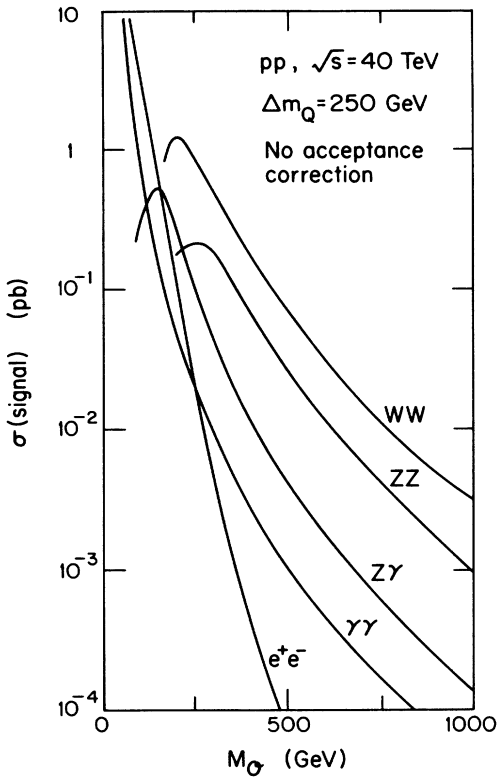

FIG. 18. Expected cross sections for gauge-boson pairs and e^+e^- pairs from quarkonium decays at the SSC as a function of the mass of the quarkonium. The $\gamma\gamma$, $Z\gamma$, and ZZ signals are almost completely from η_Q, the e^+e^- signal from ψ_Q, and W^+W^- from η_Q and ψ_Q. In this figure, we have assumed that the Higgs boson and any sequential heavy lepton are too heavy to be produced.

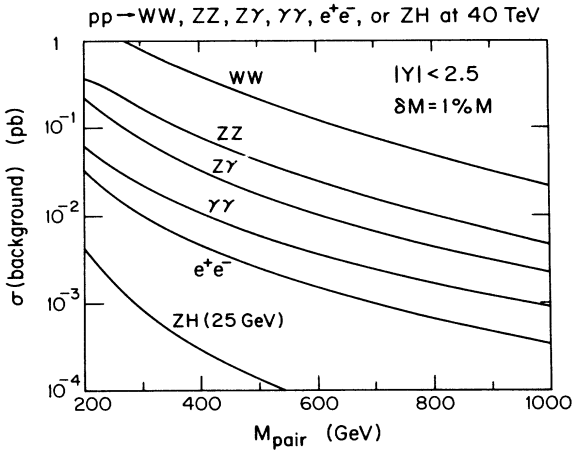

FIG. 19. The cross section $\sigma=(d\sigma/dM)\delta M$ for W^+W^-, ZZ, $Z\gamma$, $\gamma\gamma$, e^+e^-, and ZH pair production as a function of the invariant mass M of the pair at a pp collider with $\sqrt{s}=40$ TeV. The curves assume $\delta M/M=1\%$ so that the cross section shown has to be multiplied by the resolution on the measurement of the invariant mass expected for each of the processes in order to obtain an estimate of the background to the rates from quarkonium decay shown in Fig. 18.

pp center-of-mass system can be easily calculated. For the decay products of η, the acceptance (ξ) is given by[17]

$$\xi=\frac{\int_{-Y}^{Y} dy \min\left[\frac{1}{\beta}\tanh(Y-y),1\right] G(x_1)G(x_2)}{\int_{-Y_{\max}}^{Y_{\max}} dy\, G(x_1)G(x_2)}$$

with $x_{1,2}=M_{\mathcal{O}}e^{\pm y}/\sqrt{s}$, $Y_{\max}=\ln\sqrt{s}/M_{\mathcal{O}}$, $Y=\min(Y_{\text{cut}},Y_{\max})$ and β is the velocity of the produced particle. For the $\gamma\gamma$ signal, a laboratory-rapidity cut $|y|<2.5$ corresponds to an acceptance between 56% and 82% for η masses between 200 and 100 GeV. Since the η is produced with substantial rapidity ($\langle y_\eta\rangle=1.7$) in the laboratory, a cut $|y|<2.5$ leaves less than one unit of rapidity available in the rest frame of the η. The acceptance depends on the mass of the produced particles and is greater in the case of Z^0 pairs. The cross sections shown in Fig. 18 must be reduced by the appropriate acceptance factor.

The backgrounds to these signals from standard-model processes[17] are shown in Fig. 19. These depend on the attainable mass resolution; we have shown the background cross sections per percentage of mass resolution. For a mass resolution of 1%, the background from gauge-boson pairs exceeds the signal (even before reduction due to incomplete acceptance) for quarkonium masses greater than $\sim$200 GeV. Furthermore, the signal-background ratio falls rapidly with increasing quarkonium mass making the detection of heavy quarkonium more difficult.

We have further checked that it is not possible to substantially enhance the signal by reducing the acceptance in y; the signal and background change by roughly the same factor. We have also checked that a cut on the center-of-mass scattering angle (assuming $|y|<2.5$) is also not effective in enhancing the signal relative to the background.

It is possible to further enhance the signal-to-background ratio for $\mathcal{O}\to\gamma\gamma$, ZZ, and $Z\gamma$ by making a cut on the p_T of the gauge boson. The signal has a Jacobian peak at $p_T=M_{\eta/2}$ for $\eta\to\gamma\gamma$, at $p_T=(M_\eta/2)(1-M_Z{}^2/M_\eta{}^2)$ for $\eta\to Z\gamma$, and at $p_T=(M_\eta/2)(1-4M_Z{}^2/M_\eta{}^2)^{1/2}$ for $\eta\to ZZ$. For $\mathcal{O}\to W^+W^-$, it is not possible to implement this cut in practice since the p_T of each W cannot be measured, assuming we require the W to decay leptonically in order to avoid being overwhelmed by QCD background.[28] We find that while the requirement $2p_T/M_{\gamma\gamma}>0.8$ cuts out about a third of the $\eta\to\gamma\gamma$ signal, it enhances the signal-to-background ratio by about two. This enhancement is, however, not large enough to see the signal above the background. Similar conclusions also apply for the other decays of the η. We conclude, therefore, that it will be difficult to detect quarkonia via their decay into gauge-boson pairs.

The best prospect for detecting ψ heavy quarkonium is through its decay into lepton pairs. A signal-to-background ratio of $\sim$1 can be attained for a quarkonium mass $\sim$200 GeV and a mass resolution of about 3%. At

the SSC the expected cross section is ~ 0.01 pb (which corresponds to an annual rate of 100 e^+e^- events per year) from the decay of a 200-GeV quarkonium. There would be a similar rate for $\mu^+\mu^-$ events although muon momentum measurements may not be good enough to achieve this mass resolution.

B. Higgs-boson signals from quarkonium decays

(a) $H\gamma$ events. We first consider the decay $\psi \to H\gamma$. From Fig. 6(b), we see that even for the Wisconsin potential, the cross section for ψ production varies between ~ 4 pb and 10^{-1} pb as M_ψ varies from 200 to 450 GeV. Multiplying by the branching fraction for the decay $\psi \to H\gamma$ in Fig. 14, taking for illustration $M_H = 130$ GeV, the $H\gamma$ production cross section at the SSC is ~ 0.4—0.006 pb corresponding to 4000—60 events/yr. In this scenario the Higgs boson is expected to decay via $H \to t\bar{t}$. The rates for other scenarios are summarized in Table V. (The smallness of the cross section for $M_\psi = 100$ GeV is due to the reduction in the branching fraction at $M_\psi = M_Z$.) There is thus a fairly large rate for $t\bar{t}\gamma$ events, for which the invariant mass of $t\bar{t}\gamma$ peaks at M_ψ and that of $t\bar{t}$ at M_H.

(b) HZ events. Next consider a Higgs boson produced from η decay in association with the Z^0 boson. The cross section is given in Fig. 20. The standard-model background is about 2 orders of magnitude smaller than the signal, for $M_{ZH} \gtrsim 200$ GeV. The ZH rate is large for a wide range of Higgs-boson and quarkonium masses. Thus the leptonic decay of the Z^0 can be used as a trigger for the signal. If $M_H > 2M_W, 2M_Z$, the Higgs boson decays into W^+W^- and Z^0Z^0 pairs in the ratio 2:1 giving events containing three gauge bosons with an invariant mass of the η and a W^+W^- (Z^0Z^0) pair at the Higgs-boson mass. For instance, if $M_H = 240$ GeV and $M_\eta \simeq 500$ GeV, there would be about 800 $W^+W^- + (Z^0 \to l\bar{l})$ and 400 $Z^0Z^0 + (Z^0 \to l\bar{l})$ events per 10^4 pb^{-1} at the SSC.

The case of the so-called intermediate-mass Higgs boson ($2m_t < M_H < 2M_W$) is of particular interest since with only three generations the Higgs-boson signals are overwhelmed by backgrounds. If there is a fourth-generation pseudoscalar quarkonium and the decay $\eta \to ZH$ is kinematically accessible, the ZH cross section exceeds 0.5 pb if $M_\eta < 0.8$ TeV for $M_H = 130$ GeV. This corresponds to about 300 $(Z^0 \to l\bar{l}) + (H \to t\bar{t})$ events ($l = e, \mu$) per 10^4 pb^{-1} with $M_{t\bar{t}} \simeq M_H$, $M_{l\bar{l}} = M_Z$, and $M_{l^+l^-t\bar{t}} \simeq M_\eta$. If M_η is smaller ($\simeq 400$ GeV), the rate for these events may be almost an order of magnitude higher.

The dominant background to this signal comes from $Z^0t\bar{t}$ events produced by gluon fusion. The experimental resolution attainable will play a crucial role in separating the signal from background. The background has recently been studied by Gunion and Kunzst[29] and it appears that signal-to-background ratios exceeding unity can be obtained assuming reasonable mass resolutions on $M_{t\bar{t}}$ and $M_{Z^0t\bar{t}}$. Thus the decay of a fourth-generation quarkonium provides a new way of simultaneously searching for the intermediate-mass Higgs boson and the fourth generation at the SSC. Finally, consider the case $M_H < 2m_t$. If $2m_b < M_H$, the dominant decay mode of the Higgs boson would be $H \to b\bar{b}$ and it is quite likely that the signal from $\eta \to Z^0H \to Z^0b\bar{b}$ would be buried by the QCD background. One could, however, search for the subdominant decay $H \to \tau^+\tau^-$ with expected branching fractions of 3—4% since this mode leads to essentially background-free $\tau^+\tau^- + Z^0$ events; the estimated cross section of 0.03—0.3 pb corresponds to about 20—200 distinctive $l^+l^-\tau^+\tau^-$ events per year at the SSC.

(c) HH events. From Fig. 6(c) and Fig. 16 the dominant source of Higgs-boson pair production is χ_0 decay. Folding together the χ_0 production cross section with the branching fractions in Fig. 16, we obtain the Higgs-boson pair cross section shown in Table VI. Depending on the Higgs-boson mass, the events contain either four gauge bosons or four top quarks (unless $M_H < 2m_t$). For $M_H = 240$ GeV and quarkonium masses between 0.5—0.7 TeV, 10—30 four-gauge-boson events may be expected in approximate proportions $4W{:}2W2Z{:}4Z = 4{:}4{:}1$. This

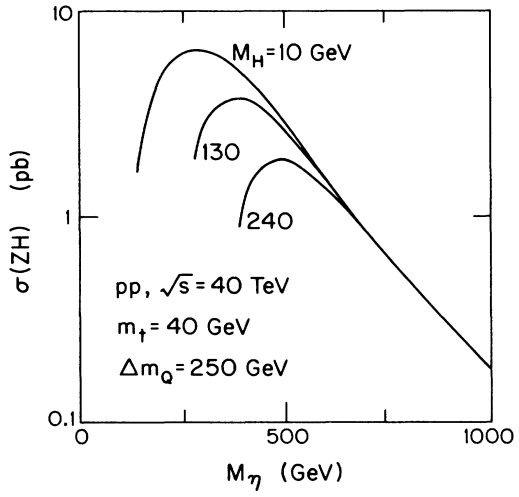

FIG. 20. The cross section for ZH production from η_Q decay at the SSC as a function of M_{η_Q} for three different Higgs-boson masses.

TABLE V. Anticipated number of $H\gamma$ pairs per 10^4 pb^{-1} integrated luminosity from ψ_Q decays.

M_ψ (GeV)	$M_H = 10$ GeV	$M_H = 130$ GeV	$M_H = 240$ GeV
100	2.9×10^3		
200	6.2×10^3	3.9×10^3	
300	8.5×10^2	7.3×10^2	3.7×10^2
400	1.6×10^2	1.5×10^2	1.1×10^2
500	42	40	33
600	13	13	11
700	5	5	5
800	2	2	2
900	1	1	1

TABLE VI. Anticipated number of HH pairs per 10^4 pb^{-1} integrated luminosity from ψ_{0Q} decays.

M_χ (GeV)	$M_H=10$ GeV	$M_H=130$ GeV	$M_H=240$ GeV
100	6.5×10^2		
200	2.7×10^2		
300	1.4×10^2	1.3×10^2	
400	78	74	
500	41	39	30
600	21	20	19
700	11	11	10
800	6	6	6
900	3	3	3

event rate is too low to be observable. In addition to these multi-gauge-boson events, the three-gauge-boson events from the decay $\eta\to ZH$ must also be present. If the mass of the quarkonium is below that of four gauge bosons, events from η decay alone would be present.

C. Heavy-lepton signals from quarkonium decays

Finally, we briefly consider the production of sequential-heavy-lepton pairs from quarkonium decay. The dominant source is η. If the decay $\eta\to ZH$ is accessible, the maximum branching fraction for $\eta\to L\bar{L}$ is about $\sim 6\%$ for $M_\eta\sim 450$ GeV [Fig. 17(b)]. Folding this with the η production cross section the event rates shown in Table VII are obtained for the production of $L\bar{L}$ pairs at the SSC. In spite of the rather substantial number of these, we do not expect that it would be possible to separate these from a comparable[17,30] (or greater) number of pairs from the Drell-Yan process. If the Higgs boson is too heavy to be produced via η decay, the branching fraction for $\eta\to L\bar{L}$ exceeds 25% for $M_\eta\simeq 700$ GeV. The increased number of $L\bar{L}$ pairs in this case are also shown in Table VII. When folded with the production cross section for the heavier η, the heavy-lepton signature is still unlikely to be separable from the Drell-Yan background. We note however, that the branching fraction for $\eta\to L\bar{L}$ increases with m_L and so the signal for heavier-lepton masses is more likely to stand out. However, since there are at least two neutrinos from the L and $\bar{L}$ decays, it is unlikely that either the L or η mass could be reconstructed. This decay is therefore unlikely to be detectable.

TABLE VII. Anticipated number of $L\bar{L}$ pairs per 10^4 pb^{-1} integrated luminosity from η_Q decays ($m_L=100$ GeV).

M_η (GeV)	$M_H=\infty$	$M_H=130$ GeV
100	0	0
200	0	0
300	1.6×10^4	1.5×10^4
400	9.8×10^3	6.9×10^3
500	5.5×10^3	2.5×10^3
600	3.5×10^3	9.8×10^2
700	2.2×10^3	4.1×10^2
800	1.5×10^3	1.7×10^2
900	1.0×10^3	76
1000	7.2×10^2	40

VI. SUMMARY AND CONCLUDING REMARKS

We have considered the possibility of discovering new heavy quarks at a multi-TeV hadron collider through the decays of their quarkonium bound states. Quarkonium states with masses less than ~ 1 TeV would be copiously produced at the proposed SSC. We focused our attention on a fourth-generation quark, although our analysis can be applied to other types of quarks such as the isosinglet quark that appears in the 27-dimensional representation of E_6. In fact, we have written most of our formulas in terms of general couplings so that they apply to any type of quark. Exceptions to this are explicitly noted.

The three aspects of our analysis are (i) production mechanisms and production rates for heavy quarkonium, (ii) decay patterns of the produced quarkonium, and (iii) a comparison of the signal and background cross sections at the SSC.

We have restricted our attention to the lowest S- and P-wave quarkonium states since these would have the largest production cross sections.

A. Quarkonium production at hadron colliders

At a hadron collider, quarkonium production occurs by $q\bar{q}$ and by gg fusion. In the range of masses of interest ($m_Q\lesssim 0.5$ TeV), the gg luminosity at the SSC exceeds the $q\bar{q}$ luminosity by a factor $\gtrsim 50$ so that it is the dominant source of quarkonium states. Even for the spin-one quarkonia ψ, χ_1, and h which do not couple to two gluons (Yang's theorem) the cross section for the process $gg\to\mathcal{O}+g$ substantially exceeds that for $q\bar{q}\to\mathcal{O}$ which takes place via electroweak interactions unless the mass of the quarkonium is very close to the Z^0 mass. In our computations, we have, therefore ignored the $q\bar{q}$ contribution to the production of quarkonium.

A crucial ingredient in the analysis is the widths for quarkonium decay to gluons. The widths are determined by the quarkonium wave functions obtained from nonrelativistic potential models. We examined the quarkonium production cross sections for various QCD-motivated quarkonium potentials that reproduce the spectroscopy of charmonium and b-quarkonium systems. Our results for these are summarized in Fig. 6.

The cross section obtained using the Cornell potential is considerably larger than those obtained using the Richardson or Wisconsin potentials. This is because the Cornell potential uses a much larger value for the coefficient of the singular term and most likely overestimates the wave functions at the origin. The cross section for the production of the pseudoscalar state η at the SSC is enormous even for the Wisconsin potential which yields the most conservative estimate. It varies between 100 pb for $M_\eta\sim 250$ GeV to ~ 0.2 pb for $M_\eta=1$ TeV. For the Richardson potential, the cross section is typically a factor of 2 larger whereas it is between a factor 20—50 larger for the Cornell potential.

The production of ψ dominantly occurs via the mechanism $gg\to\psi g$. The cross section for this is lower than the

η-production cross section by about 2 orders of magnitude.

The production of the P-wave states χ_0 and χ_2 proceeds via $gg \to \chi$. The cross sections are suppressed by 3—4 orders of magnitude relative to that for η-production because the χ radial wave function at the origin vanishes, which effectively reduces the coupling by factors of $O(k/M)$, where $k \sim$momentum of the quark inside the quarkonium and is small for a nonrelativistic system. The states χ_1 and h do not couple to two gluons and hence can only be produced via $q\bar{q}$ fusion (only χ_1) or by the bleaching gluon process. Since the cross sections for these are small they have been ignored in our analysis.

B. Decays of superheavy quarkonium

The dominant decay mode of a quark Q with a mass exceeding M_W is $Q \to W + q$. If the quarks Q and q belong to the same weak isodoublet, this decay is very rapid and dominates the decay of the quarkonium $\mathcal{O}_Q$ as can be seen from Fig. 7. If Q is the lighter of the doublet of quarks, it can only decay into a quark of another generation. For the first three generations, these mixings decrease rapidly with increasing mass and so it is plausible that a fourth-generation down-type quark may be relatively long lived. If this is indeed the case, its quarkonium states decay dominantly via annihilation (see Fig. 7). Our considerations are based on this premise. A similar situation would occur for E_6 isosinglet quarks which can only decay via mixing into the usual quarks.

In addition to the decay modes that are present for the charmonium and b-quarkonium systems, a quarkonium with a mass greater than $2M_W$ or $2M_Z$ can also decay into W^+W^-, $Z^0\gamma$, and Z^0Z^0 pairs. Furthermore if the Higgs boson is light enough the decays of quarkonium into HH, $H\gamma$, and HZ pairs may also be possible. In Sec. IV we studied the decay modes of the S- and P-wave states of heavy quarkonium and found several novel features.

For $b\bar{b}$ and $c\bar{c}$ quarkonia the dominant decays are to two gluons for spin-zero states and to three gluons for the spin-one states. From Figs. 9—12, with the exception of the η, the states of a heavy-quarkonium system dominantly decay into the weak bosons $W^\pm$ and Z^0 when the ZH mode is kinematically inaccessible. From Figs. 14—16 we see that when the Higgs boson is light enough to be produced, quarkonium decays into these are also very important. In any case, the electroweak decays into vector bosons and Higgs bosons dominate the strong decays into gluons for quarkonium masses exceeding about 0.5 TeV.

The enhancement of the weak decays was discussed in Sec. IV. This was traced to the production of longitudinal gauge bosons whose polarization vectors are of the form $k^\mu/M_V \sim M_{\mathcal{O}}/M_V$ (M_V is the vector-boson mass) for large quarkonium masses. For $M_{\mathcal{O}} \gg M_V$, the matrix elements for quarkonium decay into gauge bosons are, therefore, enhanced (unless the fermion current is conserved). This could be alternatively understood from the fact that the coupling of the longitudinal components of the gauge bosons to the quark comes from the Yukawa coupling and so is proportional to the mass of the heavy quark. The reason for the enhancements for quarkonium decay into Higgs bosons is, of course, the large Yukawa coupling to the quarks.

The enhancement factors for the various decays of the S- and P-wave quarkonium states are summarized in Table VIII. The enhancement factor for any given final state is not the same for all the quarkonia. For instance, the Z^0Z^0 decays of χ_0 and χ_2 are doubly enhanced, the ψ, h, and χ_1 singly enhanced, and the η not enhanced at all. This can be understood by studying the allowed quantum numbers for the final state as discussed in Sec. IV.

This table is a useful guide in understanding the decays of the various states. For instance, the doubly enhanced Z^0H decay of the η taken together with the enormous η production cross section leads to the novel possibility[2] of finding the intermediate-mass Higgs boson if there is a fourth generation of quarks. The signals expected at the SSC will be discussed shortly. Before closing this section

TABLE VIII. Enhancement factors for the various decays of the S- and P-wave states of heavy quarkonia. A dot denotes no enhancement whereas ↑ denotes an enhancement factor ($M_{\mathcal{O}}^2/M_W^2$). The dashes denote that the decay is absent whereas ↓ denotes a suppression. The double arrow denotes that the enhancement factor is $(M_{\mathcal{O}}^2/M_W^2)^2$. For $\eta \to L\bar{L}$ there is a chirality suppression M_L^2/M_η^2 as discussed in Sec. IV D 1 of the text.

	η	ψ	h	χ_0	χ_1	χ_2
gg	●	—	—	●	—	●
$ggg/q\bar{q}g$	●	●	●	●	●	●
$\gamma\gamma$	●	—	—	●	—	●
e^+e^-	—	●	—	—	●	—
$L\bar{L}$	↑↑	●	—	↑↑	●	—
$Z\gamma$	●	↑	↑	●	↓	●
ZZ	●	↑	↑	↑↑	↑	↑↑
W^+W^-	●	↑↑	↑	↑↑	↑	↑↑
γH	—	↑	↑	—	—	—
ZH	↑↑	↑	↑	—	↑↑	↑
HH	—	—	—	↑↑	—	↑↑

we should point out that the doubly enhanced decays $\psi \to W^+W^-$ and $\chi_1 \to ZH$ suggest the possibility of discovering these states at an electron-positron collider.[31] The production of χ_1 ($J^{PC}=1^{++}$) occurs only via Z^0 since electromagnetic interactions conserve parity. From our discussion of the decays $\mathcal{O} \to f\bar{f}$, it is clear that the other quarkonium states cannot be produced by e^+e^- collisions.

C. Superheavy-quarkonium signals at a hadron supercollider

Superheavy quarkonium can decay dominantly into vector bosons or the Higgs boson if the latter is light enough. This leads to the possibility of a variety of new signals which may be separable from standard-model processes by virtue of the fact that the decay products reconstruct to the quarkonium mass. Results for the case when the Higgs-boson mass exceeds the quarkonium mass are summarized in Fig. 18. The standard-model backgrounds are shown in Fig. 19. Assuming that the attainable mass resolution will at best be a few percent at the SSC, the prospects for identifying a heavy-quark via these decays appear to be dim in spite of the fact that each signal has cross sections in the range 0.001—1 pb. The only promising signal comes from $\psi \to e^+e^-$ for which quarks with masses up to ~ 100 GeV may be identified.

If the Higgs boson is relatively light so that quarkonium decays into it, the situation is quite different. The best prospect for simultaneously discovering the Higgs boson and a new fourth-generation quark comes from a study of the decay $\eta \to Z^0H \to l\bar{l}H$. As shown in Fig. 20, for quarkonium masses as high as 700 GeV and for $m_H < M_\eta - 250$ GeV, the ZH production cross section exceeds 1 pb; this corresponds to $\gtrsim 10^4$ Z^0H events with $M_{ZH}=M_\eta$ per year at the SSC. The large event rate allows the clean $Z^0 \to l^+l^-$ decay as a trigger. Even for the intermediate-mass Higgs boson, signal-to-background ratios exceeding unity are possible assuming reasonable experimental mass resolutions on M_{ZH} and M_H.

In addition to the ZH events just discussed, there would be ~ 100 $H\gamma$ pairs from ψ decays and a comparable number of HH pairs from χ_0 decays. Higgs-boson production from light-quark fusion is small and so the dominant background to $H\gamma$ is from $t\bar{t}\gamma$ for the intermediate-mass Higgs boson, and from $W^+W^-\gamma$ and $Z^0Z^0\gamma$ for the heavy Higgs boson. We have not estimated these backgrounds. The $H\gamma$ and HH event rates are summarized in Tables V and VI. It seems unlikely that HH pairs can be identified.

Finally, we estimate from Table VII that there could be $\sim 10^3$—10^4 heavy-lepton pairs per year at the SSC from the decay of the pseudoscalar quarkonium. This is the case for a wide range of η and Higgs-boson masses. However, it appears unlikely that these can be separated from a comparable production from the Drell-Yan process.

In summary, if there is a fourth-generation quark with small intergeneration mixings so that its weak decays are suppressed, its bound-state decays lead to interesting signals. At a multi-TeV hadron collider, these decays could lead to the identification of both the Higgs boson and a fourth-generation pseudoscalar quarkonium for a wide range of their masses.

ACKNOWLEDGMENTS

This research was supported in part by the University of Wisconsin Research Committee with funds granted by the Wisconsin Alumni Research Foundation, and in part by the U.S. Department of Energy under Contracts Nos. DE-AC02-76ER00881 and DE-FG02-84ER40173.

APPENDIX A

In this appendix we summarize the two methods used in the computation of the decay widths of the bound states.

Method 1. This technique has been previously used in Ref. 14. We include the relevant formulas here for the sake of completeness.

The amplitude for quarkonium decay into any final state can be written as a convolution of the scattering matrix element $\mathcal{O}$ into the same final state with Bethe-Salpeter wave function appropriate to the given quarkonium state. The Bethe-Salpeter wave function, in turn, is constructed in terms of the quark and antiquark spinors in a given spin configuration (triplet or singlet) and the bound-state wave function in a given orbital angular momentum state so that the total angular momentum is that corresponding to the quarkonium state. The relevant spin projectors and the resulting amplitudes for quarkonium decay have been worked out in the nonrelativistic limit, i.e., to lowest nonvanishing order in the relative momentum between the q and $\bar{q}$ in the quarkonium (we can set this equal to zero for S-wave states but must retain it to first order for P-wave states).

In terms of the quarkonium four-momentum Q, and the scattering matrix element for $q\bar{q} \to$ final state, $\mathcal{O}_F$, the decay amplitudes are given by

$$A(\eta)=\left[\frac{3}{16\pi M_\eta}\right]^{1/2} R_S(0)\mathrm{Tr}[\mathcal{O}_F\gamma_5(-\not{Q}+M_\eta)]\ , \tag{A1}$$

$$A(\psi)=-\left[\frac{3}{16\pi M_\psi}\right]^{1/2} R_S(O)\mathrm{Tr}[\mathcal{O}_F\not{\epsilon}(-\not{Q}+M_\psi)]\ , \tag{A2}$$

$$A(\chi_0)=i\left[\frac{3}{4\pi M_\chi}\right]^{1/2} R'_P(0)\mathrm{Tr}\left[\mathcal{O}_F^\alpha\left[\gamma_\alpha+\frac{Q_\alpha}{M_\chi}\right]\left[\frac{-\not{Q}+M_\chi}{2}\right]+3\mathcal{O}_F\right]\ , \tag{A3}$$

$$A(\chi_1)=\left[\frac{9}{8\pi M_\chi}\right]^{1/2}R'_P(0)\left[2\mathcal{O}_F\not{\epsilon}\gamma_5+i\epsilon^{\alpha\beta\rho\sigma}Q_\alpha\mathcal{O}_{F\beta}\gamma_\rho\epsilon_\sigma\left[\frac{-\not{Q}+M_\chi}{2M_\chi}\right]\right], \tag{A4}$$

$$A(\chi_2)=-i\left[\frac{9}{4\pi M_\chi}\right]^{1/2}R'_P(0)\epsilon_{\alpha\beta}\mathrm{Tr}\left[\mathcal{O}_F^\alpha\gamma^\beta\left[\frac{-\not{Q}+M_\chi}{2}\right]\right], \tag{A5}$$

$$A(h)=-i\left[\frac{9}{4\pi M_h}\right]^{1/2}R'_P(0)\mathrm{Tr}\left[\mathcal{O}_F\not{\epsilon}\frac{\not{Q}}{M_h}\gamma_5+\epsilon^\mu\mathcal{O}_{F\mu}\frac{\not{Q}+M_h}{2}\gamma_5\right]. \tag{A6}$$

Here, $R_S(0)$ and $R'_P(0)$ are the S-state radial wave function and the derivative of the P-state wave function, evaluated at the origin. $\mathcal{O}_F$ is the usual Feynman-diagram amplitude for a quark with momentum $Q/2+q$ and an antiquark with momentum $Q/2-q$ to scatter into the final state F, except that the spinor factors are removed. In other words, $\mathcal{O}_F$ is a product of Dirac matrices. In Eqs. (A1)—(A6), $\mathcal{O}_F$ is evaluated at $q=0$. The quantity $\mathcal{O}_F^\alpha$ that occurs in P-state decays is given by

$$\mathcal{O}_F^\alpha=\frac{\partial}{\partial q_\alpha}\mathcal{O}_F(q)\,|_{q=0}\,. \tag{A7}$$

Finally, ϵ^μ in Eqs. (A2), (A4), and (A6) is the polarization vector of the spin-one quarkonium whereas the symmetric, traceless tensor $\epsilon_{\alpha\beta}$ in Eq. (A5) satisfies

$$\epsilon_{\alpha\beta}Q^\beta=0$$

and, therefore, has five independent components as may be expected for a spin-two particle. In summing over the polarizations of χ_2, we have frequently made use of the identity

$$\sum_{\text{polarizations}}\epsilon_{\mu\nu}\epsilon_{\alpha\beta}=\tfrac{1}{2}(P_{\mu\alpha}P_{\nu\beta}+P_{\mu\beta}P_{\nu\alpha})-\tfrac{1}{3}P_{\mu\nu}P_{\alpha\beta} \tag{A8}$$

with

$$P_{\alpha\beta}\equiv-g_{\alpha\beta}+\frac{Q_\alpha Q_\beta}{M_\chi{}^2}\,.$$

The decay rates can then be obtained from the decay amplitudes as usual.

Method 2. Use of helicity amplitudes rather than the squared matrix elements facilitates the calculation when there are many diagrams. In evaluating the decay rates of quarkonium states, the helicity amplitude method explained below provides an efficient way of computation for two-body final states.

We consider two-body decays of S- and P-wave quarkonia: $\mathcal{O}(Q\bar{Q})\to 1+2$. We assume the binding is weak (binding energy $\ll$ quark mass) so that the nonrelativistic approximation can be used for the quarkonium states. Here, we give a heuristic derivation of the width formula. We start from the scattering amplitude for the process

$$Q(p,h)+\bar{Q}(\bar{p},\bar{h})\to 1(k_1,\lambda_1)+2(k_2,\lambda_2)\,. \tag{A9}$$

The momentum and helicity of each particle is shown in parentheses. We work in the c.m. frame and take the Q momentum direction as the z axis. Near the $Q\bar{Q}$ threshold

$$p=m_Q(1,0,0,\beta_Q),\quad \bar{p}=m_Q(1,0,0,-\beta_Q)\,, \tag{A10}$$

where β_Q is the velocity of the quark. We can neglect terms of $\mathcal{O}(\beta_Q{}^2)$ or higher as we will consider S and P states only.

We now rewrite the helicity amplitude in terms of definite J^{PC} states:

$$\mathcal{M}_{h\bar{h}}^{\lambda_1\lambda_2}(Q+\bar{Q}\to 1+2)=\sum_{\text{states}}\mathcal{M}_{J_z}^{\lambda_1\lambda_2}(^{2S+1}L_J\to 1+2)\mathcal{P}_{h\bar{h}}(^{2S+1}L_J)\,, \tag{A11}$$

where $J_Z=h-\bar{h}\equiv\lambda_i$, and the projectors $\mathcal{P}_{h\bar{h}}$ are given by

$$\mathcal{P}_{h\bar{h}}(^1S_0)=\frac{1}{\sqrt{2}}(-1)^{\bar{h}-1/2}\delta_{\lambda_i 0}\,, \tag{A12a}$$

$$\mathcal{P}_{h\bar{h}}(^3S_1)=|\lambda_i|+\frac{1}{\sqrt{2}}\delta_{\lambda_i 0}\,, \tag{A12b}$$

$$\mathcal{P}_{h\bar{h}}(^1P_1)=\mathcal{P}_{h\bar{h}}(^1S_0)\,, \tag{A12c}$$

$$\mathcal{P}_{h\bar{h}}(^3P_J)=(110\lambda_i\,|\,J\lambda_i)\mathcal{P}_{h\bar{h}}(^3S_1)\,, \tag{A12d}$$

or specifically,

$$\mathcal{P}_{h\bar{h}}(^3P_0)=-\frac{1}{\sqrt{6}}\delta_{\lambda_i 0}\,, \tag{A12e}$$

$$\mathcal{P}_{h\bar{h}}(^3P_1)=-\frac{1}{\sqrt{2}}\lambda_i\,, \tag{A12f}$$

$$\mathcal{P}_{h\bar{h}}(^3P_2)=\frac{1}{\sqrt{2}}|\lambda_i|+\frac{1}{\sqrt{3}}\delta_{\lambda_i 0}\,. \tag{A12g}$$

These projectors can be derived using the conventional spin wave function and with the definition

$$|J,J_Z,L,S\rangle=\sum_{L_z,S_z}(LSL_ZS_Z\,|\,JJ_Z)\,|\,L,L_Z\rangle\,|\,S,S_Z\rangle\,. \tag{A13}$$

We have fixed the initial quark direction along the z axis, thus restricting to $L_Z=0$ states. This is sufficient to obtain all the necessary amplitudes because of the rotational invariance. In Eq. (A12) we used the Condon-Shortley convention for the Clebsch-Gordan coefficients. It should be kept in mind that in calculating the helicity amplitude one should use a phase convention consistent with it, e.g., that of Jacob and Wick. It is convenient to extract from the amplitude the kinematical angular factor

$$\mathcal{M}_{J_Z}^{\lambda_1\lambda_2}(^{2S+1}L_J\to 1+2)$$
$$=4\pi\mathcal{A}^{\lambda_1\lambda_2}(^{2S+1}L_J\to 1+2)d^J_{\lambda_i\lambda_f}(\theta)e^{i(\lambda_i-\lambda_f)\phi}\ , \quad \text{(A14)}$$

where θ and ϕ are the angles of the final particle 1 and $\lambda_f=\lambda_1-\lambda_2$. Note that the amplitude $\mathcal{A}$ is independent of the magnetic quantum number $J_Z=\lambda_i$.

We can now calculate the total cross section for $Q+\bar{Q}\to 1+2$ for a definite initial state with quantum numbers $^{2S+1}L_J$. We have

$$\sigma(^{2S+1}L_J\to 1+2)=\int\frac{1}{2s\beta_Q}(2\pi)^4\delta^4(p+\bar{p}-k_1-k_2)\frac{d^3k_1}{(2\pi)^3 2k_1^0}\frac{d^3k_2}{(2\pi)^3 2k_2^0}\sum_{\lambda_1,\lambda_2}|\mathcal{M}_{J_z}^{\lambda_1\lambda_2}(^{2S+1}L_J\to 1+2)|^2$$
$$=\frac{\beta_{12}}{4M^2\beta_Q}\sum_{\lambda_1,\lambda_2}|\mathcal{A}^{\lambda_1\lambda_2}(^{2S+1}L_J\to 1+2)|^2\int[d^J_{\lambda_i\lambda_f}(\theta)]^2 d\Omega$$
$$=\frac{\pi\beta_{12}}{(2J+1)M^2\beta_Q}\sum_{\lambda_1,\lambda_2}|\mathcal{A}^{\lambda_1,\lambda_2}(^{2S+1}L_J\to 1+2)|^2\ , \quad \text{(A15)}$$

where we put $s=M^2$, and

$$\beta_{12}=[(1-R_1-R_2)^2-4R_1R_2]^{1/2}\ , \quad \text{(A16)}$$

with $R_i=M_i^2/M^2$. If the final two particles are identical, a factor of $\frac{1}{2}$ must be included. The result is independent of J_Z as expected. Note the $\beta_Q{}^{-1}$ factor which gives the characteristic behavior of an exothermic reaction at threshold (for S states).

We can relate the cross section (A15) to the decay width of corresponding quarkonium state if the binding is weak, i.e., $E_{\text{bin}}\ll m_Q$, or more rigorously, if the space-time scale of the binding force is much larger than that of the annihilation process. This condition is satisfied for decays of heavy-quarkonium states unless the Q value for the decay is very small.

The amplitude at the threshold, ($\beta_Q\to 0$), has S-wave pieces only. The decay rate of an S state is given by

$$\Gamma(^{2S+1}S_J\to 1+2)=2\beta_Q\sigma(^{2S+1}S_J\to 1+2)|\psi_S(0)|^2\ , \quad \text{(A17)}$$

where $\psi_S(0)$ is the (total) nonrelativistic wave function at the origin. This formula may be better understood in the antiquark rest frame: the factor $2\beta_Q$ is the velocity of the quark in this frame, and $|\psi_S(0)|^2$ is the number density of the quark at the antiquark. (There is no time dilation factor in our approximation.) To obtain an explicit formula we assume hereafter the final particles are colorless. Then

$$\psi_S(0)=\frac{1}{\sqrt{3}}\delta_{ij}\frac{1}{\sqrt{4\pi}}R_S(0)\ .$$

The first factor ($=\sqrt{3}$) comes from the color wave function, and the second factor is the orbital angular wave function of S states. We obtain

$$\Gamma(^{2S+1}S_J\to 1+2)=\frac{3\beta_Q}{2\pi}\sigma(^{2S+1}S_J\to 1+2)|R_S(0)|^2$$
$$=\frac{3\beta_{12}}{2(2J+1)M^2}\sum_{\lambda_1,\lambda_2}|\mathcal{A}^{\lambda_1\lambda_2}(^{2S+1}S_J\to 1+2)|^2|R_S(0)|^2\ . \quad \text{(A18)}$$

Here M^2 can be interpreted as the quarkonium mass. There is an additional factor of $\frac{1}{2}$ for identical particles. It is easy to extend this formula to the case of colored final particles. Thus the helicity amplitude at threshold is sufficient to calculate the decay width of the S-wave states. In the special case that only one state (either $^1S_0$ or $^3S_1$) can decay to the final state in consideration, the spin-averaged cross section is enough to obtain the width.

For P-wave states there is one factor of relative momentum, so we need the helicity amplitude up to $O(\beta_Q)$. There is no S-wave piece in the $O(\beta_Q)$ term. The factor β_Q is converted to the derivative of the quarkonium wave function. The conversion factor from the cross section to the width is

$$(2\beta_Q)\left|\sqrt{3}\left[\frac{3}{4\pi}\right]^{1/2}\frac{1}{\frac{1}{2}\beta_Q M}R'_P(0)\right|^2\ .$$

The factor $(3/4\pi)^{1/2}$ is the $L=1$ angular wave function, and a factor $\frac{1}{2}\beta_Q M$ has been converted into the derivative. The decay width for a P-wave state is thus

$$\Gamma(^{2S+1}P_J\to 1+2)=\frac{18}{\pi\beta_Q M^2}\sigma(^{2S+1}P_J\to 1+2)\,|\,R'_P(0)\,|^2=\frac{18\beta_{12}}{(2J+1)M^4}\sum_{\lambda_1,\lambda_2}|\,\beta_Q{}^{-1}\mathscr{A}^{\lambda_1\lambda_2}(^{2S+1}P_J\to 1+2)\,|^2\,|\,R'_P(0)\,|^2\,. \tag{A19}$$

Again a factor of $\frac{1}{2}$ for identical final particles is understood.

APPENDIX B

In this appendix we illustrate the computational techniques discussed in Appendix A by explicitly calculating the decays $\mathscr{O}\to Z^0Z^0$.

Method 1. As can be seen from Eqs. (A1)—(A6), the first step in the computation involves the calculation of the scattering matrix element $\mathscr{O}_F$ and its derivative $(\partial/\partial q_\alpha)\mathscr{O}_F(q)$. $\mathscr{O}_F$ is the usual Feynman-diagram amplitude for a quark with momentum $Q/2+q$ and an antiquark with momentum $Q/2-q$ to scatter into the final state $F\,(=Z^0Z^0$ in this example), except that the spinor factors are removed. The Feynman diagrams contributing to $Q\bar{Q}\to Z^0Z^0$ are the quark exchanges in the t and u channels and the Higgs-boson in the s channel.

For Z^0Z^0 production via the t- and u-channel exchanges we have

$$\mathscr{O}_{t+u}(q)=\left[\frac{g_Z{}^2\gamma_\mu(v_Q-a_Q\gamma_5)\left[\frac{\not Q}{2}+\not q-\not k_2+m_Q\right]\gamma_\nu(v_Q-a_Q\gamma_5)}{\left[\frac{Q}{2}+q-k_2\right]^2-m_Q{}^2}+(\mu\leftrightarrow\nu,k_1\leftrightarrow k_2)\right]\epsilon_\mu^*(k_1)\epsilon_\nu^*(k_2) \tag{B1}$$

while from the Higgs-boson exchange, we have

$$\mathscr{O}_s(q)=-\tfrac{1}{2}g_Z{}^2\frac{m_Q}{4m_Q{}^2-M_H{}^2}g_{\mu\nu}\,. \tag{B2}$$

The derivative with respect to q^α of the amplitudes can now be readily calculated. For the derivative at $q=0$, we have

$$\begin{aligned}\mathscr{O}^\alpha_{t+u}(0)=g_Z{}^2\Bigg[&\frac{v_Q{}^2+a_Q{}^2+2v_Qa_Q\gamma_5}{2m_Q{}^2-M_Z{}^2}\gamma_\mu\gamma_\alpha\gamma_\nu+2\frac{v_Q{}^2+a_Q{}^2+2v_Qa_Q\gamma_5}{(2m_Q{}^2-M_Z{}^2)^2}\gamma_\mu\left[\frac{\not Q}{2}-\not k_2\right]\gamma_\nu\left[\frac{Q}{2}-k_2\right]_\alpha\\&+\frac{2m_Q(v_Q{}^2-a_Q{}^2)}{(2m_Q{}^2-M_Z{}^2)^2}\gamma_\mu\gamma_\nu\left[\frac{Q}{2}-k_2\right]_\alpha+(\mu\leftrightarrow\nu,k_1\leftrightarrow k_2)\Bigg]\epsilon_\mu^*(k_1)\epsilon_\nu^*(k_2)\end{aligned} \tag{B3}$$

and

$$\mathscr{O}^\alpha_s(0)=0\,. \tag{B4}$$

Here k_1 and k_2 are the four-momenta of the two Z^0 bosons, v_Q and a_Q the vector and axial-vector couplings of the quarks as defined in the text, and m_Q is the mass of the quark Q. Equations (B3) and (B4) are relevant only for the computation of the decays of the P-wave states whereas (B1) and (B2) enter the computation of all the decays.

The evaluation of the amplitudes (A1)—(A6) now involves a straightforward though, at times, tedious computation of traces of products of Dirac matrices. We find that for the Z^0Z^0 decays of quarkonium the amplitudes are (we list here all the amplitudes for the Z^0Z^0 decay of S- and P-wave quarkonia)

$$A(\eta\to ZZ)=\left[\frac{3}{\pi M_\eta}\right]^{1/2}\frac{R_S(0)}{M_\eta{}^2}\frac{1}{1-2R_Z}4g_Z{}^2(v_Q{}^2+a_Q{}^2)\epsilon_\mu^*(k_1)\epsilon_\nu^*(k_2)\epsilon^{\alpha\mu\beta\nu}Q_\alpha k_{2\beta}\,, \tag{B5}$$

$$A(\psi\to ZZ)=-\left[\frac{3}{\pi M_\psi}\right]\frac{R_S(0)}{M_\psi}\frac{1}{1-2R_Z}4g_Z{}^2v_Qa_Q\epsilon_\mu^*(k_1)\epsilon_\nu^*(k_2)\epsilon_\alpha(Q)\epsilon^{\alpha\mu\beta\nu}(k_1-k_2)_\beta\,, \tag{B6}$$

$$\begin{aligned}A(\chi_0\to ZZ)=\left[\frac{3}{4\pi M_\chi}\right]\frac{R'_P(0)g_Z{}^2}{M_\chi}\Bigg[&\epsilon^*(k_1)\cdot\epsilon^*(k_2)\left[\frac{-16(v_Q{}^2+a_Q{}^2)R_Z}{(1-2R_Z)^2}+\frac{24(v_Q{}^2-a_Q^2)}{1-2R_Z}+\frac{3}{1-R_H}\right]\\&-\frac{16Q\cdot\epsilon^*(k_1)Q\cdot\epsilon^*(k_2)}{M_\chi{}^2}\left[\frac{2(v_Q{}^2+a_Q{}^2)(1-R_Z)+(v_Q{}^2-a_Q{}^2)}{(1-2R_Z)^2}\right]\Bigg]\,,\end{aligned} \tag{B7}$$

$$A(\chi_1\to ZZ)=\left[\frac{9}{8\pi M_\chi}\right]^{1/2}\frac{R_P'(0)}{M_\chi{}^2}\frac{64g_Z{}^2}{(1-2R_Z)^2}[v_Q{}^2R_Z-a_Q{}^2(\tfrac{1}{2}-R_Z)]\epsilon_\rho^*(k_1)\epsilon_\beta^*(k_2)\epsilon_\sigma(Q)\epsilon^{\alpha\beta\rho\sigma}\left[\frac{Q}{2}-k_2\right]_\alpha , \tag{B8}$$

$$A(\chi_2\to ZZ)=\left[\frac{1}{\pi M_\chi}\right]^{1/2}\frac{R_P'(0)}{M_\chi{}^4}\frac{48g_Z{}^2\epsilon^{\alpha\beta}(Q)}{(1-2R_Z)^2}\left\{(v_Q{}^2+a_Q{}^2)\left[\left[M_Z{}^2-\frac{M_\chi{}^2}{2}\right]\epsilon_\alpha^*(k_1)\epsilon_\beta^*(k_2)+k_{1\alpha}k_{1\beta}\epsilon^*(k_1)\cdot\epsilon^*(k_2)\right]\right.$$
$$\left.+v_Q{}^2[Q\cdot\epsilon^*(k_1)\epsilon_\beta^*(k_2)k_{1\alpha}-Q\cdot\epsilon^*(k_2)\epsilon_\beta(k_1)k_{1\alpha}]\right\} , \tag{B9}$$

$$A(h\to ZZ)=-\left[\frac{9}{4\pi M_h}\right]^{1/2}\frac{R_P'(0)}{M_h{}^2}\frac{16g_Z{}^2v_Qa_Q}{1-2R_Z}[Q\cdot\epsilon^*(k_2)\epsilon^*(k_1)\cdot\epsilon(Q)+Q\cdot\epsilon^*(k_1)\epsilon(Q)\cdot\epsilon^*(k_2)] . \tag{B10}$$

In the amplitudes (B6), (B8), and (B10), $\epsilon(Q)$ denotes the polarization vector of the decaying quarkonium, whereas $\epsilon_{\alpha\beta}(Q)$ in (B9) is the polarization tensor for χ_2. The amplitudes can now be readily squared to obtain the spin-averaged and spin-summed squared matrix elements. The computation of the square of the amplitude (B9) is considerably simplified by the use of the identity (A8). The decay rates for the quarkonia can now be calculated as usual.

We now turn to the helicity amplitude method for obtaining the decay rates.

Method 2. We first consider the amplitude for the t-channel quark-exchange diagram given by

$$\mathcal{M}^{(t)}=\frac{-g_Z{}^2}{(p-k_1)^2-m_Q{}^2}\bar v(\bar p)\not\epsilon_2^*(v_Q-a_Q\gamma_5)(\not p-\not k_1+m_Q)\not\epsilon_1^*(v_Q-a_Q\gamma_5)u(p) , \tag{B11}$$

where $g_Z=e/\sin\theta_W\cos\theta_W$. The amplitude $\mathcal{M}^{(u)}$ for the crossed diagram is obtained from $\mathcal{M}^{(t)}$ by exchange $\epsilon_1^*\leftrightarrow\epsilon_2^*$, $k_1\leftrightarrow k_2$. The amplitude for the s-channel Higgs-boson exchange is

$$\mathcal{M}^{(s)}=\frac{g_Z{}^2m_Q}{2(s-M_H{}^2)}\epsilon_1^*\cdot\epsilon_2^*\bar v(\bar p)u(p) . \tag{B12}$$

This last amplitude vanishes at threshold and does not contribute to the decay of S states. (It contributes to the ${}^3P_0$ state only.) The t-channel amplitude can be rewritten without any approximation:

$$\mathcal{M}^{(t)}=\frac{g_Z{}^2}{s(1-2R_Z-\beta_Q\beta_Z\cos\theta)}\{i[\epsilon_1^*\epsilon_2^*K\widetilde H]+\epsilon_1^*\cdot\epsilon_2^*K\cdot H+2(q\cdot\epsilon_1^*\epsilon_2^*\cdot H-q\cdot\epsilon_2^*\epsilon_1^*\cdot H)+(P\cdot\epsilon_1^*\epsilon_2^*\cdot H+P\cdot\epsilon_2^*\epsilon_1^*\cdot H)$$
$$-4a_Q{}^2m_Q\bar v(\bar p)\not\epsilon_2^*\not\epsilon_1^*u(p)\} , \tag{B13}$$

where $q=p+\bar p=k_1+k_2$, $P=p-\bar p$, $K=k_1-k_2$, $[ABCD]=\epsilon_{\mu\nu\rho\sigma}A^\nu B^\nu C^\rho D^\sigma$, and vectors H and $\widetilde H$ are given by

$$H^\mu=(v_Q{}^2+a_Q{}^2)\bar v(\bar p)\gamma^\mu u(p)-2v_Qa_Q\bar v(\bar p)\gamma^\mu\gamma^5u(p) ,$$
$$\widetilde H{}^\mu=-2v_Qa_Q\bar v(\bar p)\gamma^\mu u(p)+(v_Q{}^2+a_Q{}^2)\bar v(\bar p)\gamma^\mu\gamma^5u(p) , \tag{B14}$$

which are just numbers for a fixed helicity $(h,\bar h)$. The crossed amplitude is likewise

$$\mathcal{M}^{(u)}=\frac{g_Z{}^2}{s(1-2R_Z+\beta_Q\beta_Z\cos\theta)}\{i[\epsilon_1^*\epsilon_2^*K\widetilde H]-\epsilon_1^*\cdot\epsilon_2^*K\cdot H-2(q\cdot\epsilon_1^*\epsilon_2^*\cdot H-q\cdot\epsilon_2^*\epsilon_1^*\cdot H)+(P\cdot\epsilon_1^*\epsilon_2^*\cdot H+P\cdot\epsilon_2^*\epsilon_1^*\cdot H)$$
$$-4a_Q{}^2m_Q\bar v(\bar p)\not\epsilon_1^*\not\epsilon_2^*u(p)\} . \tag{B15}$$

Adding these two at threshold ($\beta_Q\to0, P\to0$) gives

$$\mathcal{M}=\frac{2g_Z{}^2}{M^2(1-2R_Z)}i[\epsilon_1^*\epsilon_2^*K\widetilde H] . \tag{B16}$$

(Note that the sum of the last terms, $\epsilon_1^*\cdot\epsilon_2^*\bar vu$, vanishes at threshold.) The vector $\widetilde H{}^\mu$ in (B14) reduces to

$$\widetilde H{}^0=(v_Q{}^2+a_Q{}^2)2m_Q(-1)^{\bar h+1/2}\chi_{\bar h}^\dagger\chi_h , \tag{B17a}$$

$$\widetilde H{}^i=-2v_Qa_Q2m_Q(-1)^{\bar h+1/2}\chi_{\bar h}^\dagger\sigma^i\chi_h . \tag{B17b}$$

Here $h,\bar h=\pm\frac{1}{2}$ is the helicity of the quark (antiquark), and χ_h is the two-component Pauli spinor for helicity h. We use the convention

$$\chi_+=\begin{bmatrix}1\\0\end{bmatrix} , \quad \chi_-=\begin{bmatrix}0\\1\end{bmatrix} .$$

The space components of $\widetilde H$ (B17b) contribute to the decay of the spin-triplet state. Using the Jacob-Wick convention for the Z polarization vectors, we obtain, for the ${}^3S_1\to ZZ$ amplitude,

$$\mathcal{A}^{\lambda_1\lambda_2}({}^3S_1\to ZZ)=\frac{4\sqrt2\,\alpha_Zv_Qa_Q}{1-2R_Z}\gamma_Z^{n_L}\beta_Z{}^2\lambda_f . \tag{B18}$$

Here $\gamma_Z = M/2M_Z$, n_L is the number of longitudinal Z in the final state (in this case $n_L = 1$). The amplitude is parity violating and only the final states with $|\lambda_f| = 1 (Z_L Z_T)$ are allowed. Inserting this amplitude (B18) into the formula (A18) for the vector state

$$\Gamma({}^3S_1 \to ZZ) = \frac{\beta_Z}{4M^2} \sum_{\lambda_1 \lambda_2} |\mathscr{A}^{\lambda_1 \lambda_2}({}^3S_1 \to ZZ)|^2 |R_S(0)|^2 \tag{B19}$$

(note a factor $\frac{1}{2}$ for identical particle is included), we can obtain the result (4.19).

The time component of $\tilde{H}$, on the other hand, is nonvanishing for the spin-singlet combination and gives the ${}^1S_0 \to ZZ$ amplitude

$$\mathscr{A}^{\lambda_1 \lambda_2}({}^1S_0 \to ZZ) = \frac{2\sqrt{2}\,\alpha_Z (v_Q{}^2 + a_Q{}^2)}{1 - 2R_Z} \gamma_Z^{n_L} \beta_Z \delta_{0\lambda_f} \lambda_1 \,. \tag{B20}$$

The amplitude is parity conserving and contains the $Z_T Z_T$ states only. The decay rate (4.18) can be readily calculated from (B10).

Finally we list the helicity amplitudes for the P states. We have

$$\beta_Q{}^{-1} \mathscr{A}^{\lambda_1 \lambda_2}({}^3P_0 \to ZZ) = (\tfrac{8}{3})^{1/2} g_Z^2 \gamma_Z^{n_L} \delta_{0\lambda_f} \left[\frac{A_{\lambda_1 \lambda_2}}{(1 - 2R_Z)^2} + \frac{B_{\lambda_1 \lambda_2}}{1 - R_H} \right], \tag{B21}$$

where

$$\begin{aligned} A_{\pm\pm} &= -(3 - 8R_Z) v_Q{}^2 + (3 - 4R_Z) a_Q{}^2 \,, \\ A_{00} &= 16 R_Z{}^2 v_Q{}^2 - 8(1 - 2R_Z)^2 a_Q{}^2 \,, \\ B_{\pm\pm} &= -\tfrac{3}{8} \,, \quad B_{00} = \tfrac{3}{4}(1 - 2R_Z) \,, \end{aligned} \tag{B22}$$

$$\beta_Q{}^{-1} \mathscr{A}^{\lambda_1 \lambda_2}({}^3P_1 \to ZZ) = \frac{4 g_Z{}^2}{1 - 2R_Z} \gamma_Z \beta_Z{}^2 \left[-\frac{2R_Z}{1 - 2R_Z} v_Q{}^2 + a_Q{}^2 \right] \lambda_f \,, \tag{B23}$$

$$\beta_Q{}^{-1} \mathscr{A}^{\lambda_1 \lambda_2}({}^3P_2 \to ZZ) = \frac{2\sqrt{2}\, g_Z{}^2}{1 - 2R_Z} \gamma_Z^{n_L} C_{\lambda_1 \lambda_2} \,, \tag{B24}$$

where

$$\begin{aligned} C_{\pm\mp} &= -2(v_Q{}^2 + a_Q{}^2) \,, \\ C_{\pm 0} = C_{0\mp} &= -\sqrt{2} \left[v_Q{}^2 \frac{2R_Z}{1 - 2R_Z} + a_Q{}^2 \right], \\ C_{\pm\pm} &= -(\tfrac{2}{3})^{1/2} (v_Q{}^2 + a_Q{}^2) \frac{2R_Z}{1 - 2R_Z} \,, \\ C_{00} &= -(\tfrac{2}{3})^{1/2} \left[v_Q{}^2 \frac{16 R_Z{}^2}{1 - 2R_Z} + 4 a_Q{}^2 (1 - 2R_Z) \right]. \end{aligned} \tag{B25}$$

Finally

$$\beta_Q{}^{-1} \mathscr{A}^{\lambda_1 \lambda_2}({}^1P_1 \to ZZ) = \frac{4\sqrt{2}\, g_Z{}^2}{1 - 2R_Z} v_Q a_Q \gamma_Z \beta_Z (-1)^{\lambda_2} |\lambda_f| \,. \tag{B26}$$

Note that only $\lambda_f = \pm 1$ (0) states are allowed for $J = 1$ (0) decays. Various enhancement factors (or suppression in the case of the vector coupling) may be explicitly seen in these amplitudes.

[1] V. Barger and A. D. Martin, Phys. Rev. D **31**, 1051 (1985).

[2] V. Barger *et al.*, Phys. Rev. Lett. **57**, 1672 (1986).

[3] W-Y. Keung, in *Proceedings of the Z^0 Physics Workshop, Ithaca, New York, 1981,* edited by M. E. Peskin and S.-H. Tye (Newman Laboratory of Nuclear Studies, Cornell University, Ithaca, 1981); E. L. Berger and D. Jones, Phys. Rev. D **23**, 1521 (1981); L. Clavelli, P. H. Cox, and B. Harms, *ibid.* **29**, 57 (1984); R. Gastmans, W. Troost, and T. T. Wu, Phys. Lett. **184B**, 257 (1987); B. Humpert, *ibid.* **184B**, 105 (1987).

[4] F. M. Renard, Z. Phys. C **1**, 225 (1979); J. H. Kühn and P. M. Zerwas, Phys. Lett. **154B**, 448 (1985); P. J. Franzini and F. J. Gilman, Phys. Rev. D **32**, 237 (1985); L. J. Hall, S. F. King, and S. R. Sharpe, Nucl. Phys. **B260**, 510 (1985); A. Martin, Phys. Lett. **156B**, 411 (1985); S. Güsken, J.-H. Kühn, and P. M. Zerwas, Nucl. Phys. **B262**, 393 (1985).

[5] C. Quigg and J. L. Rosner, Phys. Rep. **56**, 167 (1979); A. Khare, Nucl. Phys. **B152**, 533 (1979).

[6] E. Eichten, K. Gottfried, T. Kinoshita, K. D. Lane, and T. M. Yan, Phys. Rev. D **17**, 3090 (1979); **21**, 203 (1980).

[7] J. L. Richardson, Phys. Lett. **82B**, 272 (1979); W. Buchmüller and S.-H. Tye, Phys. Rev. D **24**, 132 (1981).

[8] Kaoru Hagiwara, Steve Jacobs, M. G. Olsson, and K. J. Miller, Phys. Lett. **130B**, 209 (1983); a recent analysis by K. Hagiwara, A. D. Martin, and A. W. Peacock, Z. Phys. C **33**, 135 (1986), shows $\Lambda_{\overline{\rm MS}} > 150$ MeV can be accommodated by the data. Relativistic effects are discussed in Steve Jacobs, M. G. Olsson, and Casimir Suchyta III, Phys. Rev. D **33**, 3338 (1986); **34**, 3536 (1986).

[9] See, e.g., V. A. Novikov *et al.*, Phys. Rep. **41**, 1 (1978).

[10] E. Eichten and K. Gottfried, Phys. Lett. **66B**, 286 (1977); C. Quigg and J. L. Rosner, *ibid.* **72B**, 462 (1978). For explicit results for t-quarkonium, see Franzini and Gilman (Ref. 4).

[11] V. Barger, W.-Y. Keung, and R. J. N. Phillips, Phys. Lett. **91B**, 253 (1980); Z. Phys. C **6**, 169 (1980); T. Weiler, Phys. Rev. Lett. **44**, 304 (1980).

[12] I. Bigi *et al.*, Phys. Lett. **181B**, 157 (1986); L. Bergström and P. Poutianinen, *ibid.* **182B**, 83 (1986).

[13] See, e.g., R. Baier and R. Rückl, Z. Phys. C **19**, 251 (1983).

[14] J. H. Kühn, J. Kaplan, and E. G. Safiani, Nucl. Phys. **B157**, 125 (1979); B. Guberina, J. H. Kühn, R. Peccei, and R. Rückl, *ibid.* **B174**, 317 (1980).

[15] V. Barger, H. Baer, and K. Hagiwara, Phys. Lett. **146B**, 257 (1984).

[16] D. Duke and J. F. Owens, Phys. Rev. D **30**, 49 (1984).

[17] E. Eichten, I. Hinchliffe, K. Lane, and C. Quigg, Rev. Mod. Phys. **56**, 579 (1984).

[18]M. S. Chanowitz and M. K. Gaillard, Phys. Lett. **142B**, 85 (1984); S. Dawson, Nucl. Phys. **B249**, 42 (1985); G. L. Kane, W. W. Repko, and W. B. Rolnick, Phys. Lett. **148B**, 367 (1984).

[19]K. Fujikawa, Prog. Theor. Phys. **61**, 1186 (1979); T. G. Rizzo, Phys. Rev. D **23**, 1987 (1981).

[20]V. Barger, H. Baer, K. Hagiwara, and R. J. N. Phillips, Phys. Rev. D **30**, 947 (1984).

[21]T. P. Cheng and L.-F. Li, Phys. Rev. D **34**, 226 (1986).

[22]B. Pendleton and G. G. Ross, Phys. Lett. **98B**, 291 (1981); C. Hill, Phys. Rev. D **24**, 691 (1981); M. Machacek and M. T. Vaughn, Phys. Lett. **103B**, 427 (1981); J. Bagger, S. Dimopoulos, and E. Masso, Nucl. Phys. **B253**, 397 (1985); J. W. Halley, E. A. Paschos, and H. Usler, Phys. Lett. **155B**, 107 (1985).

[23]J. H. Kühn, Acta Phys. Pol. **B12**, 347 (1981). This paper contains some of the widths presented here including the widths of heavy quarkonia to Z^0 and H.

[24]The QCD corrections to the following decays have been calculated: $\psi \to l\bar{l}$, R. Barbieri *et al.*, Nucl. Phys. **B105**, 125 (1976); W. Celmaster, Phys. Rev. D **19**, 1517 (1979); $\eta \to gg$, R. Barbieri *et al.*, Nucl. Phys. **B154**, 535 (1979); K. Hagiwara *et al.*, *ibid.* **B177**, 461 (1981); $\psi \to ggg$, P. B. Mackenzie and G. P. Lepage, Phys. Rev. Lett. **47**, 1244 (1981); $\chi \to gg, \gamma\gamma$, R. Barbieri *et al.*, Phys. Lett. **95B**, 93 (1980); Nucl. Phys. **B192**, 61 (1981); Phys. Lett. **106B**, 497 (1981); $\psi \to H\gamma$, M. I. Vysotsky, *ibid.* **97B**, 159 (1980); P. Nason, *ibid.* **175B**, 233 (1986).

[25]J. Kaplan and J. H. Kühn, Phys. Lett. **78B** 252 (1978).

[26]F. Wilczek, Phys. Rev. Lett. **39**, 1304 (1977).

[27]K. Gottfried, Phys. Rev. Lett. **40**, 598 (1978); T.-M. Yan, Phys. Rev. D **22**, 1652 (1980); Y.-P. Kuang and T.-M. Yan, *ibid.* **24**, 1974 (1981); C. A. Flory and I. Hinchliffe, Phys. Lett. **107B**, 139 (1981).

[28]W. J. Stirling, R. Kleiss, and S. D. Ellis, Phys. Lett. **163B**, 261 (1985).

[29]J. F. Gunion and Z. Kunzst, University of California—Davis Report No. 86-21, 1986 (unpublished).

[30]If the sequential lepton mass is large ($\gtrsim$200 GeV) it can also be produced from a gluon fusion through a quark loop at a rate exceeding that from the Drell-Yan production. For a discussion of this, see S. S. D. Willenbrock and D. A. Dicus, Phys. Lett. **156B**, 429 (1985).

[31]The $^1P_1$ state cannot be produced since $\Gamma(^1P_1 \to f\bar{f})$ is zero.